



## The Estimation of Water Quality Parameters in Lentic Environments Through Remote Sensing Technologies: a Review of the Past Two Decades

*Estimativa de Parâmetros de Qualidade da Água em Ambientes Lênticos Por Meio de Tecnologias de Sensoriamento Remoto: uma Revisão das Últimas Duas Décadas*

Fernanda Mara Coelho Pizani<sup>1</sup>, Philippe Maillard<sup>2</sup> e Camila Costa Amorim<sup>3</sup>

<sup>1</sup> Federal University of Minas Gerais, Belo Horizonte, Brazil. [fm.coelho@yahoo.com.br](mailto:fm.coelho@yahoo.com.br)  
ORCID: <https://orcid.org/0000-0001-8841-8193>

<sup>2</sup> Federal University of Minas Gerais, Belo Horizonte, Brazil. [philippermaillard@yahoo.com.br](mailto:philippermaillard@yahoo.com.br)  
ORCID: <https://orcid.org/0000-0003-3405-5096>

<sup>3</sup> Federal University of Minas Gerais, Belo Horizonte, Brazil. [camila@desa.ufmg.br](mailto:camila@desa.ufmg.br)  
ORCID: <https://orcid.org/0000-0001-6132-0866>

Received: 04.2022 | Accepted: 06.2022

**Abstract:** The use of remote sensing technology applied to measure the quality of continental waters has grown exponentially since the turn of the century. Using different sensors on board satellites or airborne platforms, the estimation of water quality parameters has been carried out through both empirical and analytical approaches. This work aims to review the specific scientific production of the last two decades to assess how the evolution of the sensors and platforms have affected the potential and the limitations of remote sensing technologies to estimate water quality parameters in lakes and reservoirs. The study also focuses on the accuracy of remote sensing techniques for the major optically active parameters: chlorophyll-a and phycocyanin, Secchi disk depth and turbidity. The article is subdivided by sections dedicated to each of these parameters. A review of remote sensing platforms and sensors precedes the parameters sections. The past 20 years have brought a large body of articles on how remote sensing data can be used to estimate these parameters. Empirical methods dominate overwhelmingly with a four to one proportion over analytical approaches. Environmental factors such as season, complexity of water and concentration loads appear to exert a strong control over the quality of the results. Recent platforms and sensors have brought noticeable improvements over results achieved in this period.

**Keywords:** Water Quality. Optical Sensors. Satellite Missions. Empirical Models. Analytical Models.

**Resumo:** O uso da tecnologia de sensoriamento remoto aplicada para mensurar a qualidade das águas continentais tem crescido exponencialmente desde a virada do século. Usando diferentes sensores a bordo de satélites ou plataformas aéreas, a estimativa dos parâmetros de qualidade da água vem sendo realizada por meio de abordagens empíricas e analíticas. Este trabalho visa revisar a produção científica específica das últimas duas décadas para avaliar como a evolução dos sensores e plataformas afetaram o potencial e as limitações das tecnologias de sensoriamento remoto para estimar parâmetros de qualidade da água em lagos e reservatórios. O estudo também se concentra na precisão das técnicas de sensoriamento remoto para os principais parâmetros opticamente ativos: clorofila-a e ficocianina, profundidade do disco de Secchi e turbidez. O artigo está subdividido em seções dedicadas a cada um desses parâmetros. Uma revisão das plataformas e sensores de sensoriamento remoto precede as seções de parâmetros. Os últimos 20 anos trouxeram uma grande quantidade de artigos sobre como os dados de sensoriamento remoto podem ser usados para estimar esses parâmetros. Os métodos empíricos predominam com uma proporção de quatro para um sobre as abordagens analíticas. Fatores ambientais como estação do ano, complexidade das cargas de água e concentração parecem exercer um forte controle sobre a qualidade dos resultados. Plataformas e sensores recentes trouxeram melhorias notáveis em relação aos resultados alcançados neste período.

**Palavras-chave:** Qualidade da Água. Sensores Ópticos. Missões de Satélites. Modelos Empíricos. Modelos Analíticos.

## 1 INTRODUÇÃO

Monitoring water quality (WQ) in aquatic lentic environments is critical for the proper management of

water resources and to guarantee a sustainable use. It is also a means to get an insight on the dynamics of the surrounding human activities (ODERMATT et al., 2008). The quality of these environments can be determined through their physical, chemical and biological characteristics which will be addressed as WQ “parameters”.

There are hundreds of parameters that can attest the quality of water. Some of the most common parameters that can be monitored remotely are chlorophyll-a (chl-a), transparency, turbidity and total suspended matters (TSM) (AVDAN et al., 2019). In addition to these parameters, remote sensing has been used to estimate coloured dissolved organic matter (CDOM), phycocyanin (PC), true colour and temperature. Other non-optically active parameters can also be inferred indirectly through their relationship with the optically active ones: total phosphorous (TP) (XIONG et al., 2019), total nitrogen (TN) (LIU et al., 2015), pH, chemical oxygen demand (COD) and dissolved oxygen (DO) (WANG et al., 2012; WANG et al., 2014; PU et al., 2019). Time series of satellite images have also been used to monitor surface water temperature (ALCÂNTARA et al., 2011; CURTARELLI et al., 2014; LUZ; GUASSELLI; ROCHA, 2017), an important parameter not only for WQ but also as a means to monitor climatic changes (LI et al., 2017).

Much of the literature on the topic of remote sensing applied to WQ can be found in periodical articles from the past forty years with a few books also dedicated to the subject. Liu, Islam and Gao (2003) did an extensive review on the subject going as far back as 1981 and covering up until the year 2000. Since then, there has been an increased number of publications in these past two decades boosted by the emergence of a large number of new satellite missions with better spectral and spatial resolution and by the explosion of the number of accessible unmanned aerial vehicles (UAV), drones and small high performance multispectral and hyperspectral cameras. These new platforms and sensors have received much attention as means to acquire WQ estimates remotely.

Remote sensing applied to WQ has been investigated by a variety of scientific communities such as hydrology (POTES; COSTA; SALGADO, 2012; CURTARELLI et al., 2014; BONANSEA et al., 2015; HANSEN; WILLIAMS, 2018), hydrobiology (ZHANG et al., 2016; BRESCIANI et al., 2018), public health (TORBICK et al., 2014; VAN DER MERWE; PRICE, 2015; TORBICK et al., 2018), urban planning (HUO et al., 2014; LIU et al., 2015) and applied statistics (WILKIE et al., 2019; LI; HUANG; WANG, 2020), amongst others. Whatever the application or the purpose, most authors have brought forward the relative ease and low cost of remote sensing methods over traditional in situ methods (BONANSEA et al., 2015; ABDELMALIK, 2018; AVDAN et al., 2019). Furthermore, it has been reported that these traditional approaches often use a relatively small number of samples and at an insufficient frequency (WILKIE et al., 2019). Within that context, remote sensing can bring a comprehensive distributed estimate of some important WQ parameters (STEFOULI; CHAROU, 2012) even considering some important limitations like the restriction to the surface layer and several other uncontrolled factors affecting the optical properties of water like the atmospheric conditions at the moment of acquisition and the interference of the air-water interface (for a review, see Mertes et al. (2004)).

The advantages mentioned above are well recognized and have transformed remote sensing in a widely used tool for monitoring lakes and reservoirs. Lentic environments suffer constant threats mainly characterised by changes in water level, toxic pollution, salinization, eutrophication, acidification, sediment pollution and invasion from exotic species, which all contribute to the deterioration of the quality of water (ODERMATT et al., 2018). A wide range of approaches have been applied to this aim: empirical, semi-empirical, analytical and semi-analytical. Whereas empirical methods focus on establishing a statistical relationship between the values of some WQ parameter and the corresponding radiance or reflectance measured by optical sensors, analytical methods are based on radiative transfer equations to model how the physical properties of absorption and dispersion of light are altered by such parameter (VAN NGUYEN et al., 2020). Some approaches blend the two methods by incorporating prior knowledge (for instance by pre-selecting spectral bands) or by fine-tuning an analytical approach through some adjustment method (e.g., regression, root mean square error).

Other empirical approaches include machine learning (HUO et al., 2014; RUESCAS et al., 2018; KUPSSINKU et al., 2020; PAHLEVAN et al., 2020) and artificial neural network (ANN) (FERREIRA; GALO, 2013; VERONEZ et al., 2018; PU et al., 2019) that showed good potential for estimating chl-a and CDOM. Ha et al. (2017) successfully used ANN to determine the level of eutrophication in lakes. It is within the context of reporting the advancements achieved in the past two decades in terms of platforms, sensors and

data processing that this article has been prepared. Firstly, we present an overview of the remote sensing instruments (sensors and platforms) used to monitor WQ, then we investigate each of the most common optically active WQ parameters and how remote sensing technology has been successfully used for their determination.

## 2 INSTRUMENTS USED IN AQUATIC REMOTE SENSING

Remote sensing applied to aquatic applications allows to make time series of observations about the quality of surface water of lakes, reservoirs and rivers and their dynamics (ZHANG et al., 2016). Some remote sensing platforms and instruments also allow to assess the quantity of water through altimetry sensors (ROSMORDUC et al., 2018) but this aspect will not be treated here. The effectiveness of the application of remote sensing to estimate WQ depends on the choice of appropriate platforms and instruments for this purpose. Optical sensors measure the amount of electromagnetic radiation at different wavelengths reflected by the aquatic surface. The data are usually converted in radiance or reflectance before being used to estimate WQ parameters (ALPARSLAN; COSKUN; ALGANCI, 2009). In particular, the reflectance measurements (which are independent from the amount of illumination) are fundamental for the generation of WQ models based on remote sensing (LI et al., 2020).

The past twenty years (2000 – 2020) have been marked by the development of new instruments (platforms and sensors) capable of improved measurement estimates of surface or near-surface WQ parameters, some of which were specifically designed for such purpose. Advances in these sensors include finer spectral, spatial and radiometric resolutions, shorter revisit time, increased number of satellite constellations, and the possibility of free and easily retrieved data. The scientific community has proven the effectiveness of using these sensors for the evaluation of various processes including many environmental parameters (ALPARSLAN; COSKUN; ALGANCI, 2010). Estimates of WQ in lentic environments by remote sensing can be performed at local, regional, continental or global scales (see Politi, Cutler and Rowan (2015)). Depending on the research objective, one can choose from a broad variety of platforms (Table 1).

Satellite images covering the visible and infrared spectral regions present a discretised brightness signal that combines the radiance of the surface and the interference of the atmosphere between the surface and the sensor. Pre-processing is then required to reduce the effect of the atmosphere on the data (ABDELMALIK, 2018). Molecules in the atmosphere and aerosols absorb and scatter both the incoming solar radiation and outgoing radiance reflected by the Earth' surface and alter the signal that reaches the sensor, a process generally called atmospheric attenuation (ANSPER; ALIKAS, 2019). The process of atmospheric attenuation is well understood today and a wealth of algorithms are available to correct these effects on the different satellite sensors for which many review articles are available (SOLA et al., 2018; ZHANG et al., 2018; DOXANI et al., 2018; MISHRA et al., 2020). The most sophisticated of these algorithms use complementary information (often from other satellites or meteorological models) such as aerosol thickness, water vapour and digital elevation models to improve the correction. Some sensors have incorporated specific bands like the “coastal / aerosol”, “water vapour” and “cirrus” bands (bands 1, 9 and 10) of the Sentinel-2 multispectral Instrument (MSI) in order to improve atmospheric correction.

Most moderate and high spatial resolution satellite images are freely available through satellite agencies like the United States Geological Survey (USGS) Earth Explorer (<https://earthexplorer.usgs.gov/>) or the European Space Agency/Copernicus' Copernicus Open Access Hub (<https://scihub.copernicus.eu/>). Very-high-resolution images can also be obtained from commercial satellites, but can be excessively expensive depending on the size of the area. In the case of models using in situ data conjugated with satellite image data it is highly recommended to match the field campaign with the passage of the satellite to ensure more accurate results and to avoid the effect of changes in the environmental conditions that could alter the WQ parameters (CHEN et al., 2016).

Table 1- Satellites and airborne vehicles sensors launched between 2000 and 2009 often used for WQ assessment.

Legend: AHS=Airborne Hyperspectral Scanner.

Platform/Sensor	Launch date	Spectral bands (nm)	Spatial resolution (m)	Temporal resolution (days)
EO-1/ALI	Nov 2000	6 VNIR (433-890); 1 Pan (480-690); 3 SWIR (1200-2350)	10-30	16
EO-1/Hyperion	Nov 2000	242 Hyperspectral bands: 49 VNIR (426-925); 147 SWIR (912-2395). 22 bands are not calibrated, have no valid values and are not included into Earth Engine assets	30	16
NOAA-16/AVHRR	Sep 2000	2 VNIR (580-1110); 1 SWIR (1580-1640); 1 MWIR (3550-3930); 2 TIR (10300-12500)	1100-4000	9
DigitalGlobe/ Quickbird	Oct 2001	4 VNIR (430-918); 1 Pan (450-900)	2.62-0.65	2.5
PROBA-1/CHRIS	Oct 2001	19 VNIR (400 - 1050)	18 - 36	7
AHS/CASI-1500	2002	288 Hyperspectral bands: VNIR (380-1050)	0.25-5	-
ENVISAT/AATSR	Mar 2002	3 VNIR (555-865); 1 SWIR (1600); 1 MWIR (3700); TIR (10850-12000)	1000	3-6
ENVISAT/MERIS	Mar 2002	15 VNIR (390-1040)	300-1200	3
SPOT-5/HRG	May 2002	3 VNIR (500-890); 1 Pan (480-710); 1 SWIR (1580-1750)	2.5 or 5-10-20	26
CBERS-2-2B/CCD, IRMSS, IRS and WFI	Oct 2003, Sep 2007	WFI: 2 VNIR (630-890) CCD: 1 Pan (510-730) 3 VNIR (450-890) IRMSS: 1 Pan (510-1100) 2 SWIR (1550-2350) 1 TIR (10400-12500)	20  80 or 160  2.7	5  26 (nadir) 3 (off-nadir)  26
CBERS-3-4/MUX, PAN, IRS and WFI	Dec 2013, Dec 2014	MUX: 4 VNIR (450-890) PAN: 1 Pan (510-850) 3 VNIR (520-890) IRS: 1 Pan (500-900) 2 SWIR (1550-2350) 1 TIR (10400-1250) WFI: 4 VNIR (450-890)	20  5 or 10  40 or 80  64	26  5  26  5
CBERS-04A/WPM, MUX and WFI	Dec 2019	WPM: 1 Pan (450-900) 4 VNIR (450-890) MUX: 4 VNIR (450-890) WFI: 4 VNIR (450-890)	2 or 8  16.5  55	31  31  5
CARTOSAT/Pan	May 2005	1 Pan (500-850)	2.5	5
ALOS/AVNIR-2	Jan 2006	4 VNIR (420-890); 1 Pan (520-770)	2.5-10	2
DigitalGlobe/ WorldView-1	Sep 2007	1 Pan	0.5	1.7

(To be continued)

(Conclusion)

<b>Platform/Sensor</b>	<b>Launch date</b>	<b>Spectral bands (nm)</b>	<b>Spatial resolution (m)</b>	<b>Temporal resolution (days)</b>
RapidEye/REIS	Aug 2008	5 VNIR (440-850)	5	1 (off-nadir) 5.5 (nadir)
HICO/International Space Station	Sep 2009	128 Hyperspectral bands: VNIR (350-1080)	100	10
DigitalGlobe/WorldView-2	Oct 2009	8 VNIR (400-1040); 1 Pan (450-800)	1.85-0.46	1.1
COMS/GOCI	Jun 2010	8 VNIR (400-865)	500	10 image per day: 8 day, 2 night
GeoEye/GeoEye-1	Sep 2010	8 VNIR (450-920); 1 Pan (450-800)	1.65-0.41	< 3
AHS/APEX-ESA	2011	> 300 Hyperspectral bands: Default 114 VNIR (380-970); 199 SWIR (940-2500)	2-5	–
Suomi NPP/VIIRS	Oct 2011	5 bands (640-1145); 16 Moderate-res. bands (412-12013); 1 Day/Night band (500-900)	375-750	1-2 times a day
AHS/AVIRIS-NG	2012	425 Hyperspectral bands: (380-2510)	0.3-4	-
AHS/AisaFENIX	2013	620 Hyperspectral bands: VNIR (380-970); SWIR (970-2500)	1 m at 600 m altitude	-
Landsat-8/OLI and TIRS	Feb 2013	5 VNIR (430-880); 1 Pan (500-680); 2 SWIR (1570-2290); 1 Cirrus Cloud Detection (1360-1380); 2 TIR (10600-12510)	30-15-100	16
AHS/HySpex ODIN-1024	2014	427 Hyperspectral bands: VNIR (400-1000); SWIR (950-2500)	0.5 m at 2000 m altitude	-
NOAA/ WorldView-3	Aug 2014	8 VNIR (400-1040); 1 Pan (450-800); 8 SWIR (1195-2365)	1.24-3.7-0.31	1 - 4.5
Sentinel-2A-2B/MSI	Jun 2015, Mar 2017	8 VNIR (490-865); 2 SWIR (1610-2190); 3 atmospheric correction bands (443-1375)	10-20-60	10
Sentinel-3A-3B/OLCI	Feb 2016, Apr 2018	21 VNIR (400-1020)	300-1200	< 2.8
DigitalGlobe/WorldView-4	Nov 2016	4 VNIR (655-920); 1 Pan (450-800)	0.3-1.24	1-4.5
PRISMA	2008– Latest: Mar 2019	238 Hyperspectral bands: 66 VNIR (400-1010); 1 Pan (400-700); 171 SWIR (920-2505)	5-30	29
GEO-KOMPSAT-2B/GOCI-II	Feb 2020	1 UV (370-390); VNIR (412-755); 1 Pan (845-885)	250	10 times a day

Source: Adapted from Gholizadeh et al. (2016).

Many recent multispectral and hyperspectral sensors were especially constructed for use in atmospheric platforms like aeroplanes, helicopters and UAVs. The latter have been widely popularised in recent years for remote sensing use, mostly fuelled by the availability of light weight sensors. The choice of platform is mostly dictated by the size of the area and the speed of the platform (VAN DER MERWE; PRICE, 2015). A variety of airborne sensors have been used for remote sensing of WQ, like the APEX, the MIVIS and the HySpex (PINARDI et al., 2015). These are still relatively large and heavy equipment and can only be carried by manned aircraft or high-end drones. Table 2 shows some of the characteristics of these sensors. Images from these sensors

allow a synoptic view of small- to medium-sized water bodies that can be monitored under different weather and water conditions with extremely high spatial and spectral resolution (SABAT-TOMALA et al., 2018). However, the high cost of scheduled field campaigns can be considered an adverse factor for their use.

Table 2 - Some of the main specifications of three hyperspectral sensors: APEX, MIVIS and HySpex.

Sensor	Spectral range	Number of bands	Spectral resolution (nm)	FOV (°)	I FOV (°)	Pixels (width)
APEX	VNIR: 380-970 SWIR: 940-2500	VNIR: 334 SWIR: 199	VNIR: 0.6-6.3 SWIR: 7-13.5	28	0.028	1024
MIVIS	I: 430-830 II: 1150-1550 III: 2.0-2.5 VI: 820-1270	I: 20 II: 50 III: 8 VI: 450	I: 20 II: 8 III: 64 VI: 10	71.1	0.114	755
HySpex	400-800 430-820 485-960 400-1000	72-88	5.5	16-40	0.016-0.039	1024

Source: Authors (2021).

UAVs have been considered a good alternative for remote sensing studies of the aquatic environment. These vehicles are often characterised as being multi-rotors or fixed-wing. The multi-rotor UAVs are normally slower than fixed-wing ones. Most multi-rotor UAVs have a battery autonomy limited to 30~minutes to a couple of hours depending on the model and payload but have the advantage of flying at lower altitudes and are able to hover while the fixed-wing can be more efficient due to their higher speed and can cover larger areas in less flight time (VAN DER MERWE; PRICE, 2015). The cameras on-board aircraft can capture images in extremely high spatial resolution, reduce revisit time, allow access to difficult areas for boats, have a lower cost than in situ campaigns and laboratory analysis and suffer less from atmospheric attenuation (KUPSSINKU et al., 2020). There are today quite a range of light weight (many under 1 kg) multispectral and hyperspectral cameras especially build for those more accessible drones (especially RGB, like Canon ELPH 110HS and Powershot S100). Although the multispectral and hyperspectral sensors on the market are relatively costly (ranging from USD 10,000 to USD 40,000), some low-cost compact sensors can also be purchased (VERONEZ et al., 2018), all depending on the ultimate goal of the research.

Conversely, because drones operate in the lower layer of the atmosphere, they are subject to significant turbulence and data collected by drones need to suffer correction and calibration that can be difficult to apply. Satellites travel at speed in excess of 6000 m.s<sup>-1</sup> whereas drones are in the range of 10 – 30 m.s<sup>-1</sup> with the consequence that the time lag of the survey flights can imply differences in illumination and atmospheric conditions. Even if the camera is calibrated at the beginning and end of every flight, in practice it is a very complex logistic. By flying below clouds, one could think that this gives drone an advantage over satellites but in reality, the illumination changes provoked by clouds and cloud shadow can be very difficult to compensate. Problems of glare are also common depending on the sun elevation. Finally, it should be mentioned that in most cases, the ultra-high resolution achieved through drones is not necessarily an advantage as WQ phenomenon are usually characterised by a much lower operational scale.

### 3 OPTICALLY SIGNIFICANT WATER CONSTITUENTS

This section is dedicated to the following optically active WQ parameters: chlorophyll-a (chl-a) and phycocyanin (PC), Secchi disk depth (SDD) and turbidity.

#### 3.1 Concentration of Chlorophyll-a (Chl-a) and Phycocyanin (PC)

Phytoplankton communities represent one of the WQ parameters that can be better detected and monitored by remote sensors. The analysis of the trophic state and WQ of a lake or reservoir is related, among

other factors, to the abundance of phytoplankton (BRESCIANI et al. 2020). The increase concentration of these species is a major cause of water contamination (PEPPA; VASILAKOS; KAVROUDAKIS, 2020). High nutrient loads (nitrogen and phosphorus) accelerate the growth and biomass production of algae (PYO et al., 2018) and can be associated with phytoplankton blooms (WILKIE et al., 2019). There is real concern about cyanotoxins blooming in water bodies as these toxins pose an effective threat to public health. Detection via remote sensing of these algal blooms in continental waters, which could contain harmful cyanobacteria, has been based on the remote estimate of chl-a and PC (OGASHAWARA, 2019).

Usually, cyanobacterial blooms appear in the morning due to the respiratory process that occurs during the absence of light, which explains the disappearance of these blooms in the afternoon and reappearance in the morning (BRESCIANI et al., 2018). Seasonal factors such as temperature rise and wind dynamics also influence the distribution, abundance and diversity of phytoplankton species (BRESCIANI et al., 2020). The time of emergence of blooms (morning) favours the use of optical remote sensing to estimate this parameter through its relationship with chlorophyll. There is a difference in the absorption and reflection of light between water with predominant concentration of phytoplankton (Case 1) and more complex water, with high levels of turbidity, CDOM and TSM (Case 2) (MALAHLELA et al., 2018). Several authors indicate the appropriateness of using algorithms like the blue/green band ratio for Case 1 (BINDING et al., 2011; WATANABE et al., 2018; ANSPER; ALIKAS, 2019; ZENG; BINDING, 2019) while the use of bands in the NIR and red regions are more applicable to the waters of Case 2, since the interference of the non-algal particle response and CDOM are reduced considerably in these regions (CHENG et al., 2013). In addition to the blue/green and NIR/red ratios to estimate the concentration of chl-a, studies often adopt a third algorithm based on spectral curvature that uses a three-band ratio: Fluorescence Line Height (FLH, which uses one band centred at 685 nm) and Maximum Chlorophyll Index (MCI, which uses a central band at 706 nm) are examples of this kind of algorithm (FLORES-ANDERSON et al., 2020).

The quantification of chl-a and PC is also possible through hyperspectral imaging. The diversity of bands of sensors like Hyperion (satellite EO-1) and CHRIS (Proba-1) allows for the application of more than 100 hyperspectral indices for providing good estimates of chl-a concentrations, achieving robust results through a four-band algorithm (Normal Chlorophyll Index – NCI, using the 550 nm, 675 nm, 690 nm and 700 nm bands) (CHENG et al., 2013). The Hyperion sensor also proved useful for complex systems with low chl-a concentrations ( $<10 \text{ mg/m}^3$ ) (FLORES-ANDERSON et al., 2020). The AisaFENIX instrument from Specim (<https://www.specim.fi/>) has proved superior to the previous ones in WQ studies: coupled with specific atmospheric correction techniques, the sensor obtained very good performance in the quantification of chl-a from a eutrophic lake using a semi-analytical algorithm (NIR/red) (MARKELIN et al., 2017).

Although demanding higher logistic costs because of the aerial campaigns, images from MIVIS and APEX sensors were also able to validate 3D numerical hydrodynamic models of lakes, identifying potential algal blooms using semi-empirical band ratio approaches for both MIVIS (677 nm, 710 nm and 747 nm) as for APEX (670 – 673 nm and 690 – 697 nm) (PINARDI et al., 2015). Sensors on-board UAVs are capable of registering very high and ultra-high resolution images, both spatially and spectrally. The visible and NIR bands from the PIKA-L hyperspectral sensor were used to estimate chl-a and had its results compared with the products of two other sensors: the WorldView-3 multispectral and the Airborne Hyperspectral Scanner (AHS) presenting, among them, the best performance (EUGENIO; MARCELLO; MARTÍN, 2020).

Over the past twenty years, new sensors have been developed and tested to estimate chl-a and PC. VHR multispectral images, such as WorldView-2 (FERREIRA; GALO, 2013) and WorldView-3 (EUGENIO; MARCELLO; MARTÍN, 2020) were used with average results. Although the sensors have very fine spatial resolution, the spectral resolution of these sensors is often less refined. The results presented in the study involving WorldView-3 were a slightly better but still the data were not able to adequately capture the spatial variation of chl-a.

Products from the Landsat series are among the high-resolution images capable of quantifying chl-a and PC. Although the TM and ETM+ sensors have been extensively used in the last few decades (NOVO et al., 2013; OGASHAWARA et al., 2014b; HANSEN; WILLIAMS, 2018), the OLI sensor on-board Landsat-8 has been used since its launch in 2013, replacing the old sensors with better results through empirical models (WATANABE et al., 2015; MALAHLELA et al., 2018).

With the advent of the MSI instrument on-board the Sentinel-2 mission, noticeable improvement was achieved for chl-a estimates in view of the new bands in the red-edge region and its high spatio-temporal resolution (the red-edge bands have a spatial resolution of 20 m and the S-2A and -2B combined enable the acquisition of an image every five days). Studies show that empirical algorithms that associate chl-a and the green-red band ratio showed a strong correlation with data collected in situ (HA et al., 2017). For these estimates, two, three and four band algorithms were also successfully employed (HA et al., 2017; ANSPER; ALIKAS, 2019; PEPPA; VASILAKOS; KAVROUDAKIS, 2020; SÒRIA-PERPINYÀ et al., 2020). Some studies have simultaneously investigated the performance of the OLI and MSI sensors for quantifying chl-a, and showed good results for both, considering that these sensors were not designed exclusively for observing the optical constituents of water (BRESCIANI et al., 2018; WATANABE et al., 2018; PIZANI et al., 2020).

Part of another Copernicus mission, the Sentinel-3 is equipped with the OLCI sensor that has been specifically studied for the detection of chl-a and PC, either by using semi-empirical algorithms (OGASHAWARA, 2019) or by semi-analytical modelling (ZENG; BINDING, 2019). The instrument can be effective in quantifying the values of chl-a and PC due to its exclusive band centred at 620 nm, like its predecessor (MERIS), widely used and efficient for the development of bio-optical algorithms (OGASHAWARA, 2019). Together, the MSI and OLCI sensors have been integrated in recent scientific research. Although they present different characteristics, comparative analyses of their performance in lentic environments using machine learning algorithms suggest chl-a could be estimated with very similar accuracy from both sensors (PAHLEVAN et al., 2020). Models selected by optical classes of water bodies presented relevant results indicating MSI as slightly superior (SOOMETTS et al., 2020). By focusing on the characteristics of the two sensors, (BRESCIANI et al., 2020) achieved a better understanding of the dynamics of phytoplankton at different time and space scales in a shallow, turbid and eutrophic lake.

Most of the above mentioned studies are listed in Table 3. Because of the large number of articles, we have restricted the list to the period 2014 – 2020. Table 4 gives a quick summary of these studies.

Table 3 - Sample of remote measurements of chl-a applied to lakes and reservoirs in the last two decades with level of accuracy obtained. Legend: L-5=Landsat-5/TM, L-8=Landsat-8/OLI, S-2=Sentinel-2/MSI, S-3=Sentinel-3/OLCI, RE=RapidEye/REIS, AHS=Airborne Hyperspectral Scanner, A/MODIS=Aqua/MODIS, T/MODIS=Terra/MODIS, E/A/ML=Empirical/Analytical/Empirical based on Machine Learning

Authors	Study Area	Platform/sensor	E/A/ML	Performance evaluation
Kupssinskü et al. (2020)	Unisinós lake; Broa's Reservoir (Brazil)	S-2 UAV/Canon ELPH 110HS	ML	Mean values for the evaluated metrics: Unisinós: $r^2=0.90$ , $MSE=0.005 \mu\text{g/L}$ ; Broa's: $r^2=0.82$ , $MSE=0.005 \mu\text{g/L}$
Pahlevan et al. (2020)	Optically diferente waters (10 countries)	S-2 S-3	ML	Mixture Density Network S-2: $RMSE=30.31 \mu\text{m}^3$ , $MAPE=24\%$ S-3: $RMSE=26.98 \mu\text{m}^3$ , $MAPE=23$
Uudeberg et al. (2020)	51 lakes (Estonia and Finland)	S-2 S-3	E	S-2: $r^2=0.85$ ; S-3: $r^2=0.86$
Flores-Anderson et al. (2020)	Lake Atitlan (Guatemala)	EO-1	E	$r^2=0.70$ , $RMSE=2.005 \text{mg/m}^3$
Soomets et al. (2020)	4 Baltic lakes (Estonia and Latvia)	S-2 S-3	E	S-2: $r^2=0.84$ , $RMSE=10.49 \text{mg/m}^3$ ; S-3: $r^2=0.83$ , $RMSE=9.79 \text{mg/m}^3$
Li et al. (2020)	Donghu lake (China)	L-8	ML	$MSE=17.81$
Eugenio et al. (2020)	Maspalomas lagoon (Spain)	WV-3 AHS UAV/Pika-L	A	WV-3: $RMSE=6.75 \mu\text{g/L}$ ; AHS: $RMSE=6.65 \mu\text{g/L}$ ; UAV: $RMSE=3.49 \mu\text{g/L}$
Van Nguyen et al. (2020)	Lake Kasumigaura (Japan)	MERIS	E	$r=0.89$ , $RMSE=6.37 \text{mg/m}^3$
Sòria-Perpinyà et al. (2020)	Albufera of València lagoon (Spain)	S-2	E	Calibration: $r^2=0.84$ ; Validation: $r^2=0.77$ , $RMSE=141.0 \mu\text{g/L}^1$
Peppas, Vasilakos and Kavrouidakis (2020)	Lake Pamvotis (Greece)	S-2	E	MCI and MPH (Maximum Peak-Height): Pearson's r values up to 0.95
Bresciani et al. (2020)	Lake Trasimeno (Italy)	S-2 S-3	A	Combination of S-3 and S-2 data: Cross-validated $r^2=0.97$

(To be continued)



(Continuation)

Authors	Study Area	Platform/ sensor	E/A/ ML	Performance evaluation
Neil et al. (2019)	185 global inland and coastal aquatic systems	MERIS	E/A/ ML	Variability unknown: (E) $r=0.88$ , $RMSE=0.256 \text{ mg/m}^3$ ; Predominantly clear water/oligotrophic: (E) $r=0.82$ , $RMSE=0.306 \text{ mg/m}^3$ ; Blue to green water/mesotrophic: (E) $r=0.88$ , $RMSE=0.256 \text{ mg/m}^3$ ; Green or brown water/hypereutrophic: (A) $r=0.87$ , $RMSE=0.267 \text{ mg/m}^3$
Zeng and Binding (2019)	Lake Winnipeg & Erie (Canada)	S-3	E	$r^2=0.97$ , $RMSE=6.0 \text{ mg/m}^3$
Ogashawara (2019)	Lake Erie (USA)	S-3	E	PC > 50 $\mu\text{g/L}$ : $r^2=0.22$ , $RMSE=207.167 \mu\text{g/L}$ ; Chl-a > 50 $\mu\text{g/L}$ : $r^2=0.38$ , $RMSE=107.585 \mu\text{g/L}$
Wilkie et al. (2019)	Lake Balaton (Hungary)	MERIS	A	$RMSE=0.445 \text{ mg/m}^3$ , $MAE=0.355 \text{ mg/m}^3$
Elhag et al. (2019)	Baysh Dam (Saudi Arabia)	S-2	E	$r^2=0.96$ , $RMSE=0.039628 \text{ mg/m}^3$
Ansper and Alikas (2019)	Estonian inland lakes (Estonia)	S-2	E	Results varied according to the water type: $r^2=0.20$ to $r^2=0.97$
Hansen and Williams (2018)	Deer Creek Reservoir; Jordanelle Reservoir; Utah Lake (USA)	L-5 L-7	E	Reservoirs whole season: $r^2=0.12$ , $RMSE=24.7 \mu\text{g/L}$ ; Early season: $r^2=0.54$ , $RMSE=1.5 \mu\text{g/L}$ ; Mid season: $r^2=0.32$ , $RMSE=5.4 \mu\text{g/L}$ ; Late season: $r^2=0.73$ , $RMSE=23.7 \mu\text{g/L}$ Utah Lake whole season: $r^2=0.50$ , $RMSE=55.2 \mu\text{g/L}$ ; Early season: $r^2=0.99$ , $RMSE=1.2 \mu\text{g/L}$ ; Late season: $r^2=0.88$ , $RMSE=14.4 \mu\text{g/L}$
Bresciani et al. (2018)	Lake Maggiore; Lake Como; Lake Iseo; Lake Idro; Lake Garda (Italy)	L-8 S-2	A	Mean values: $r^2=0.82$ , $RMSE=0.43 \text{ mg/m}^3$
Blix et al. (2018)	Lake Balaton (Hungary)	S-3	ML	$r^2=0.83$ , $NRMSE=0.1042 \text{ mg/m}^3$
Bonansea, Rodrigues and Pinotti (2018)	Río Tercero Reservoir (Argentina)	L-5 L-7 L-8	E	$r^2=0.89$ , $NRMSE=18.8 \mu\text{g/L}$
Odermatt et al. (2018)	24 lakes and multiple reservoirs (4 continents)	MERIS	E/ ML	Global results: (E) $r=0.64$ , $MAE=7.726 \text{ mg/m}^3$ ; (ML) $r=0.59$ , $MAE=2.447 \text{ mg/m}^3$
Pyo et al. (2018)	Baekje Reservoir (South Korea)	AHS	A	PC: $r^2=0.77$ , $RMSE=14.90 \text{ mg/m}^3$ ; Chl-a: $r^2=0.53$ , $RMSE=10.88 \text{ mg/m}^3$
Markogianni et al. (2018)	Trichonis Lake (Greece)	L-8	E	Log chl-a: $r^2=0.33$ , Std. Err.= $0.12 \mu\text{g/L}$ ; chl-a: $r=0.44$ , $r^2=0.19$ , Std. Err.= $0.13 \mu\text{g/L}$
Binding et al. (2018)	Lake Winnipeg (Canada)	MERIS	E	$r^2=0.83$ , p-value < 0.01
Torbick et al. (2018)	New England lakes (USA)	L-7 L-8	A	$r^2=0.86$ , $RMSE=11.92 \mu\text{g/L}$
Watanabe et al. (2018)	Barra Bonita Reservoir (Brazil)	L-8 S-2	E	L-8: $r^2=0.22$ , $RMSE=84.95 \text{ mg/m}^3$ ; S-2: $r^2=0.76-0.85$ , $RMSE=69.24-127.41 \text{ mg/m}^3$

(To be continued)

(Conclusion)

Authors	Study Area	Platform/ sensor	E/A/ ML	Performance evaluation
Sabat-Tomala et al. (2018)	Zegrze Reservoir (Poland)	Cessna 402B Aeroplane/ HySpex scanner	E	$\rho=0.43$
Malahlela et al. (2018)	Vaal Dam (South Africa)	L-8	E	$r^2=0.61$
Coelho et al. (2017)	3 reservoirs: Marengo, Pau Branco, São Nicolau (Brazil)	L-8 RE	E	L-8 all reservoirs: $r^2=0.13-0.28$ , NSE=-3.89 to -0.45; RE all reservoirs: $r^2=0.20-0.40$ , NSE=-0.40 to 0.71 $\mu\text{g/L}$
Markelin et al. (2017)	Loch Leven Lake (UK)	AHS (AisaFENIX)	A	RMS=5.87 $\text{mg/m}^{-3}$
Philipson et al. (2016)	Lake Vänern (Sweden)	MERIS	E	$r=0.85$ , MAE=0.9 $\mu\text{g/L}$
Barrett and Frazier (2016)	Lake Eufaula (USA)	L-5 L-7	E	Chl-a: $r=-0.154$ ; lnChl-a: $r=-0.155$
Toming et al. (2016)	11 lakes (Estonia)	S-2	E	Chl-a TOA: $r^2=0.83$ ; Chl-a BOA: $r^2=0.80$
Torbick and Corbiere (2015)	Lake Champlain (USA)	L-8 Proba-1 RE	E	Chl-a: L-8: $r^2=0.77$ , RMSE=0.41 $\mu\text{g/L}$ ; Proba-1: $r^2=0.88$ , RMSE=0.54 $\mu\text{g/L}$ ; RE: $r^2=0.81$ , RMSE=1.46 $\mu\text{g/L}$ ; PC: L-8: $r^2=0.83$ , RMSE=1.33 $\mu\text{g/L}$ ; Proba-1: $r^2=0.88$ , RMSE=1.02 $\mu\text{g/L}$ ; RE: $r^2=0.77$ , RMSE=1.52 $\mu\text{g/L}$
Watanabe et al. (2015)	Barra Bonita Reservoir (Brazil)	L-8	E	Values varied between: $r^2=0.39$ and $r^2=0.75$
Politi, Cutler and Rowan (2015)	European lakes: Vänern, Vättern, Geneva, Balaton	Aqua/MODIS Terra/MODIS	E	Aqua/Terra: $r^2=0.014$ ; Terra: $r^2$ ranging from $r=0.76$ to $0.79$ in oligotrophic lakes
Palmer et al. (2015a)	Lake Balaton (Hungary)	MERIS	E	FLH: $r^2=0.87$ , RMSE=4.19 $\text{mg/m}^3$ ; MCI: $r^2=0.69$ , RMSE=6.62 $\text{mg/m}^3$
Palmer et al. (2015b)	Lake Balaton (Hungary)	MERIS	E	Values varied between: $r^2=0.58$ and $r^2=0.84$
Xiang et al. (2015)	Chaohu Lake (China)	Terra/MODIS	E	Values varied between: $r^2=0.57$ and $r^2=0.89$ , MSE=5.3452 and MSE=10.4689
Ogashawara and Moreno-Madriñá (2014)	Lake Thonotosassa (USA)	MODIS	E	$r^2$ and RMSE by quarter: Jan-Mar: 0.53, 45.2 $\mu\text{g/L}$ ; Apr-Jun: 0.56, 112.08 $\mu\text{g/L}$ ; Jul-Sep: 0.67, 62.02 $\mu\text{g/L}$ ; Oct-Dec: 0.06, 27.16 $\mu\text{g/L}$
Mishra and Mishra (2014)	15 aquaculture ponds (USA)	MERIS	E	Full-range PC model: $r^2=0.99$ , MRE=30.71% Model for PC < 300 $\mu\text{g/L}^{-1}$ : $r^2=0.65$ , MRE=38.18%
Ogashawara et al. (2014a)	Itumbiara Hydroelectric Reservoir (Brazil)	Terra/MODIS	E	OC2: $r^2=0.10$ , RMSE=37.03%; OC3: $r^2=0.19$ , RMSE=44.02%
Torbick et al. (2014)	4453 lakes (USA)	L-5	E	Regression coefficient=0.045, Std. Error=0.024, p-value=0.0678
Huo et al. (2014)	Water bodies in Xi'na City (China)	L-7	ML	$r^2=0.97$ , MAD=9.533 $\text{mg/L}$
Coelho et al. (2011)	Lago do Amor Reservoir (Brazil)	CBERS/CCD	E	Best result: Normalized Ratio Aquatic Vegetation Index (NRAVI) $r^2=0.91$

Source: Authors (2021).

Table 4 - Summary of Chlorophyll-a/Phycocyanin studies.

Most successful sensors		Best bands & indices	Limitations	Other comments
Low res.	High res.			
S-3, MERIS, MODIS	S-2, L-8, L-5	Blue/green, NIR/red (case 2 water), RE/red, narrow 620 nm (red), 3-and 4-band algo.	Complex water (case 2) can be very challenging. Higher concentrations might be necessary for using NIR & RE bands	High spectral resolution is more critical for chl-a. Hyperspectral can be an advantage. Normalised versions of the indices might be better.

Source: Authors (2021).

### 3.2 Secchi Disk Depth (SDD) and Transparency

The Secchi disk is a circular instrument with a diameter measuring between 20 and 30 cm, usually black and white, attached to a measuring tape and dedicated to the vertical measurement of the water transparency through immersion. The reading is made by an observer who determines the depth at which the disk seems to disappear below the water surface (LIU et al., 2019). SDD is widely used due to easy interpretation and application (TORBICK et al., 2014). This measurement is based on a theory of under-water visibility (VUNDO et al., 2019). Light attenuation implies in greater or lesser water clarity which depends directly on the concentration of suspended substances (SABAT-TOMALA et al., 2018), such as phytoplankton, organic and inorganic matter, and the proportion of clear water (LIU et al., 2019). The best time to estimate this parameter is around noon (AVDAN et al., 2019) but a correction factor can be applied to correct for sun elevation (VERSCHUUR, 1997).

The water transparency assessment represents an important factor in the monitoring and management of water resources (BONANSEA et al., 2015) for many reasons. Activities within the watershed can affect water transparency due to the carrying of sediments loads and nutrients (RODRIGUES et al., 2017). The algae proliferation process can modify the water clarity and reaches its peak in late summer, which is the period most propitious for lakes and reservoirs to show smaller SDD values (KNIGHT; VOTH, 2012).

Monitoring water transparency by remote sensing can be effective and offer advantages such as the possibility of creating models based on satellite images with only a few sampling points surveyed in the field (KNIGHT; VOTH, 2012). The main remote sensing algorithms applied to estimate SDD in the last twenty years were based on empirical or semi-analytical relationships (LIU et al., 2019).

Turbidity is a parameter that contains optical properties similar to SDD properties and, in some cases, may allow the same spectral bands combination to be used to estimate SDD (AVDAN et al., 2019). Red and blue regions of the electromagnetic spectrum are widely used to assess water clarity. The reflectance in the red band is directly proportional to the increase in turbidity, while the blue band responds inversely in proportion to the optical properties of substances that promote greater water turbidity (KNIGHT; VOTH, 2012). Combinations of visible bands (red, green and blue) have often been used in the construction of algorithms for SDD estimates in optically complex continental water (MANCINO et al., 2009; STEFOULI; CHAROU, 2012; RODRIGUES et al., 2017; VUNDO et al., 2019).

Remote sensing models with good levels of significance for SDD estimation have been applied to MODIS (LIU et al., 2019; VUNDO et al., 2019) and MERIS products (KNIGHT; VOTH, 2012; XIANG et al., 2015; POLITI; CUTLER; ROWAN, 2015; ZHANG et al., 2016) in large water bodies (>160 ha), a restriction dictated by the low spatial resolution of these sensors (KNIGHT; VOTH, 2012; LIU et al., 2019).

Images from Landsat sensors (TM, ETM+ and OLI) were used to measure SDD in multiple scientific research, providing satisfactory predictive relationships for specific studies ( $r^2 > 0.66$ ) in lakes and reservoirs (MANCINO et al., 2009; HUO et al., 2014; TORBICK et al., 2014; BONANSEA et al., 2015; XU et al., 2018). Comparing the results of the algorithms applied to the images of the OLI and MSI sensors using an analytical approach, Rodrigues et al. (2017) found that the response from OLI outperformed that of MSI products attesting its applicability in oligo-mesotrophic waters.

Recent studies have used an approach guided by optical types of water and using data from the MSI and OLCI sensors in order to compare their results and showed a high correlation between MSI sensor data

and SDD values (SOOMETTS et al., 2020; UUDEBERG et al., 2020). Although the MSI sensor has been designed mostly for terrestrial monitoring, current research shows that the development of specific algorithms and methods produced good results using data from this sensor (SOOMETTS et al., 2020).

Studies that measure SDD from optical sensors have a relatively high level of success (Table 5) in part because SDD is a direct consequence of all optical characteristics of water and the elements it contains. The summary is presented in Table 6.

Table 5 - Sample of remote measurements of SDD applied to lakes and reservoirs in the last two decades and level of accuracy obtained. Legend: L-5=Landsat-5/TM, L-8=Landsat-8/OLI, S-2=Sentinel-2/MSI, S-3=Sentinel-3/OLCI, RE=RapidEye/REIS, AHS=Airborne Hyperspectral Scanner, A/MODIS=Aqua/MODIS, T/MODIS=Terra/MODIS, E/A/ML=Empirical/Analytical/Empirical based on Machine Learning

Authors	Study Area	Platform/ sensor	E/A/ ML	Performance evaluation
Uudeberg et al. (2020)	51 Baltic lakes (Estonia and Finland)	S-2 S-3	E	S-2: $r^2=0.83$ ; S-3: $r^2=0.82$
Soomets et al. (2020)	4 Baltic lakes (Estonia and Latvia)	S-2 S-3	E	S-2: $r^2=0.97$ , RMSE=0.36 m; S-3: $r^2=0.69$ , RMSE=1.10 m
Avdan et al. (2019)	Borabey Dam (Turkey)	RE	E	$r=-0.86$
Liu et al. (2019)	Lake Taihu (China)	MERIS	A	$r^2=0.73$ , MAPD=37%
Vundo et al. (2019)	Lake Malawi (Malawi)	MERIS	A	Lee15 algorithm: $r=0.66$ , RMSE=1.17 m; Doron11 algorithm: $r=0.65$ , RMSE=3.68 m
Xu et al. (2018)	Lake Liangzi (China)	L-7 L-8	E	Estimated vs In situ measured (2016): $r^2=0.66$ , RMSE=0.118 m Long-term trend (2007-2016): $r^2=0.35$ , p-value < 0.001
Sabat-Tomala et al. (2018)	Zegrze Reservoir (Poland)	AHS	E	$\rho=0.52$
Rodrigues et al. (2017)	Nova Avanhandava Reservoir (Brazil)	L-8 S-2	A	L-8 (QAAv5 algorithm): Values between MAPE=12,86% and MAPE=31,17% S-2 (QAAM14 algorithm): Values between MAPE=14,33% and MAPE=39,13%
Politi, Cutler and Rowan (2015)	Vänern Lake; Vättern Lake; Geneva Lake (European continent)	A-T/MODIS	E	Best results Geneva Lake A-T: $r=0.245$ Aqua: $r=-0.317$ Terra: $r=0.789$ Best results Vänern and Vättern Lakes A-T: $r=-0.542$ Aqua: $r=-0.871$ Terra: $r=0.924$ Best results all lakes A-T: $r=-0.230$ Aqua: $r=-0.667$ Terra: $r=0.308$
Xiang et al. (2015)	Chaohu Lake (China)	T/MODIS	E	Values between $r^2=0.57$ and $r^2=0.89$ , MSE=5.3452 and MSE=10.4689
Bonansea et al. (2015)	Río Tercero Reservoir; Los Molinos Reservoir (Argentina)	L-5 L-7	E	$r^2=0.81$ , RMSE=0.64 m
Giardino et al. (2014)	Lake Garda (Italy)	L-8 RE	A	L-8 and RE: $r=0.72$
Torbick et al. (2014)	4453 lakes (USA)	L-5	E	Regression coefficient=-0.921, Std. Error=0.231, p-value=0.0001
Huo et al. (2014)	Water bodies in Xi'an City (China)	L-7	ML	$r^2=0.98$ , MAD=0.736 m

Source: Authors (2021).

Table 6 - Summary of SDD studies.

Most successful sensors		Best bands & indices	Limitations	Other comments
Low res.	High res.			
S-3, MERIS, MODIS	S-2, L-8, L-7, L-5	Red & blue, visible bands	Subjective, measurements may differ by operator. Should be corrected to compensate sun elevation & atmospheric condition	Easy to acquire field data, easy to interpret.

Source: Authors (2021).

### 3.3 Turbidity

Turbidity is an optically active property of water that indicates the presence of particles in the water column that can provoke the scattering or absorption of light (POTES; COSTA; SALGADO, 2012; AVDAN et al., 2019). This is an important WQ indicator (QUANG et al., 2017) adopted by most monitoring programs (ODERMATT et al., 2018). Turbidity can be caused by the presence of matter of phytoplanktonic origin and an increase in turbidity can be associated to the number of plant pigments in the water column (SABAT-TOMALA et al., 2018). Materials of mineral origin from soil erosion also contribute to water turbidity (MENKEN; BREZONIK; BAUER, 2006). Notwithstanding the specific characteristics of each indicator, TSM and turbidity can be considered directly correlated parameters (ODERMATT et al., 2008).

Turbidity is more frequently observed in stable lentic environments with low water flow (SABAT-TOMALA et al., 2018). High levels of turbidity imply lesser water transparency and can cause imbalances and damage to biological organisms (QUANG et al., 2017). The effects of turbidity can be represented by the change and evolution of the temperature measured on the water surface (POTES; COSTA; SALGADO, 2012). Turbidity can be quantified by nephelometry or estimated by SDD through observations from the surface (QUANG et al., 2017). However, Secchi’s observations may present greater uncertainties when compared to other instrumental measurement methods (SON; WANG, 2019).

Although considered an effective method, the use of remote sensing for estimating WQ parameters in complex continental aquatic environments, with high levels of turbidity is still a challenge (ROBERT et al., 2017). The use of the red spectral range in single band algorithms can produce extremely consistent and robust models for turbidity in highly turbid water using high-resolution sensors, such as Landsat-OLI (QUANG et al., 2017). However, ratio models of two or more spectral bands are more commonly used. The two-band models using the 412 nm and 560 nm wavelengths showed good estimates with low spatial resolution images from MERIS (POTES; COSTA; SALGADO, 2012), as well as using high-resolution images from the MSI (ELHAG et al., 2019) and REIS (AVDAN et al., 2019) sensors combining the green and red bands. Good results were also obtained with hyperspectral data from HySpex scanner adopting the red-edge ranges at 705 nm and 714 nm (SABAT-TOMALA et al., 2018). In general, the literature indicates that a good accuracy in turbidity prediction is possible using visible bands (SILVA et al., 2020) and the combination of visible and infrared bands (ALPARSLAN; COSKUN; ALGANCI, 2010). Good results are described with both empirical and analytical models but the choice of spectral regions for the development of turbidity estimation algorithms may also be dependent on the season, especially in eutrophic environments (BARRETT; FRAZIER, 2016). Table 7 shows a sample of studies from the last decade while Table 8 presents the turbidity summary .

Table 7 - Sample of remote measurements of turbidity applied to lakes and reservoirs in the last two decades and level of accuracy obtained. Legend: L-5=Landsat-5/TM, L-8=Landsat-8/OLI, S-2=Sentinel-2/MSI, S-3=Sentinel-3/OLCI, RE=RapidEye/REIS, AHS=Airborne Hyperspectral Scanner, A/MODIS=Aqua/MODIS, T/MODIS=Terra/MODIS, E/A/ML=Empirical/Analytical/Empirical based on Machine Learning

Authors	Study Area	Platform/sensor	E/A/ML	Performance evaluation
Facco et al. (2021)	Itaipu Reservoir (Brazil)	L-8	E	Best results: r <sup>2</sup> =0.94 (red band) r <sup>2</sup> =0.91 (NDTI)

(To be continued)

(Conclusion)

Authors	Study Area	Platform/ sensor	E/A/ ML	Performance evaluation
Silva et al. (2020)	Alton Water Reservoir (UK)	L-8 S-2	ML	Waveleat Artificial Neural Networks: NMSE=0.01404, MSE=0.00885
Avdan et al. (2019)	Borabey Dam (Turkey)	RE	E	r=0.93
Son and Wang (2019)	Great Lakes (USA/Canada)	SNPP/VIIRS	A	r=0.93
Elhag et al. (2019)	Baysh Dam (Saudi Arabia)	S-2	E	r <sup>2</sup> =0.94, RMSE=0.077774 NTU
Abdelmalik (2018)	Qaroun Lake (Egypt)	ASTER	E	r <sup>2</sup> =0.99, RMSE=0.891 NTU
Odermatt et al. (2018)	24 lakes and multiple reservoirs (4 continents)	MERIS	E	r=0.74, MAE=0.88 NTU
Sabat-Tomala et al. (2018)	Zegrze Reservoir (Poland)	AHS	E	ρ=0.54
Quang et al. (2017)	Thuy Trieu Lagoon; Cam Ranh Bay (Vietnam)	L-8	E	r <sup>2</sup> =0.84, RMSE=0.28 NTU
Barrett and Frazier (2016)	Lake Eufaula (USA)	L-5 L-7	E	Turbidity: r=N/A; lnTurbidity: r=0.43
Potes, Costa and Salgado (2012)	Alqueva Reservoir (Portugal)	MERIS	E	r=0.96, RMSE=3.62 NTU
Alparslan, Coskun and Alganci (2010)	Darlik Dam (Turkey)	L-5	E	r=0.92
Alparslan, Coskun and Alganci (2009)	Küçükçekmece Lake (Turkey)	L-5 IRS-1C/D LISS SPOT	E	r <sup>2</sup> =0.82

Source: Authors (2021).

Table 8 - Summary of turbidity studies.

Most successful sensors		Best bands & indices	Limitations	Other comments
Low res.	High res.			
MERIS	ASTER, S-2, L-8, L-7, L-5	Red (only), green/blue, visible bands, RE, NIR	The greater the turbidity, the shallower the estimate. Turbidity affects measurements of other parameters like chl-a and CDOM	Highly turbid water can produce good models with only the red band.

Source: Authors (2021).

#### 4 SCIENTIFIC AND TECHNOLOGICAL ADVANCEMENTS IN THE PAST TWO DECADES

Some of the biggest advances in studies involving aquatic remote sensing have been cloud computing and storage platforms that facilitate large-scale remote sensing analysis. Improved computing power has allowed for faster and more complex data analysis. Technologies such as Google Earth Engine (GEE), Amazon Web Services (AWS) and Siemens Xcelerator are examples of cloud-based computing platforms that can allow processing of big data for which the computational cost is usually high, a frequent problem in processing large number of image and other remote sensing data (SAGAN et al., 2020).

For remote sensing data, GEE is arguably the cloud computing platform that best serves intense users (MACIEL et al., 2021). GEE is a remote sensing information portal launched in 2010 that consists in a data catalogue providing time series of satellite images from various missions as well as vector data allowing to apply processing algorithms developed by the user or the remote sensing community (GORELICK et al., 2017; KUMAR; MUTANGA, 2018). Especially in the last five years, a number of studies have been carried out using GEE to monitor WQ parameters such as TSM (MARKERT et al., 2018; CAO et al., 2019; CABALLERO; NAVARRO, 2021), SDD (PAGE; OLMANSON; MISHRA, 2019; LIU et al., 2020) and chl-a (LIN et al., 2018; WANG et al., 2020; CABALLERO; NAVARRO, 2021; LOBO et al., 2021).

Machine Learning (ML) is an approach based on AI (Artificial Intelligence) increasingly applied to develop self-learning algorithms that can handle large number of variables from which a “characteristic” behaviour can be determined (RUSSELL; NORVIG, 1995; SAGAN et al., 2020). By definition ML needs example data or past experience and is therefore empirical and can handle non-parametric distributions of data. In addition, ML can be dynamic and adapt itself over time as new data is brought in (KIM et al., 2014; LARY et al., 2016; ALPAYDIN, 2020). It can be used to solve problems of classification, pattern recognition, outlier detection, and regression among other applications and can do both supervised and unsupervised learning (ALPAYDIN, 2020). Because ML algorithms are generally the result of “mining” large data base and using large number of variables, they are considered more robust than pure regression approaches (HAFEEZ et al., 2019). In a study involving eight lakes in Midwestern United States, Sagan et al. (2020) found that ML approaches yielded the best overall results for a number of WQ parameters including TSM, turbidity and chl-a. ML generally needs large amount of data to be efficient, and this can be a limitation in WQ applications which typically use limited amount of data unless carried out over many lakes or rivers at once.

There are a number of ML algorithms that can be used to assess WQ through remote sensing techniques, some of which are: Support Vector Regression (SVR), Gaussian Processes Regression (GPR), self-organising map (SOM), artificial neural networks, Random Forest, genetic algorithms, among others (LARY et al., 2016; PU et al., 2019; ZHANG et al., 2020). Even though ML algorithms have shown to perform well for studies involving WQ models, they can suffer from problems such as excessive dimensionality and overfitting (KUPSSINSKU et al., 2020). In addition, the type of distribution of the entry data and their associated uncertainties can strongly affect the accuracy of the results (PAHLEVAN et al., 2020).

In WQ studies, one limitation often comes from the relative scarcity of in situ data worldwide (HEAL et al., 2021). The difficulty of acquiring in situ data often results in relatively small sample sizes being used for calibrating and validating WQ models (TOPP et al., 2020). Recent years have seen the emergence of large and even global data base of WQ in situ data made accessible to the scientific community that have contributed toward the development of more generic WQ models. These data base can be invaluable for the validation and calibration of models developed for the quality of continental waters. The GEMStat Water Program is one such global data portal of the United Nations Environment Program (UNEP) hosted by the GEMS/Water Data Center (GWDC) of the International Centre for Water Resources and Global Change (ICWRGC), Koblenz, Germany (UNEP, 2021; HEAL et al., 2021). Through the portal <https://gemstat.org/>, it is possible to access WQ data from more than 75 countries on rivers, lakes and wetlands (TOPP et al., 2020). In the European Union, the Copernicus Global Land Service (CGLS), which is part of the Copernicus land monitoring program is a platform hosted by the European Commission Joint Research Centre (JRC) that provides sensor and in situ data on turbidity, trophic state index and reflectance of the aquatic surface of lakes with a spatial resolution of 100 m (Europe and Africa, from the MSI/Sentinel-2 sensor), 300 m and 1 km (global data, from the MERIS/ENVISAT and OLCI/Sentinel-3 sensors). In addition to WQ data, the portal provides information on lake surface temperature and water level (CGLS, 2021). In partnership with the United States Geological Survey (USGS), the Environmental Protection Agency (EPA), the National Water Quality Monitoring Council (NWQMC) and more than 400 state, federal, local and tribal agencies, the Water Quality Portal (WQP) is a collaborative service that provides information from more than 297 million WQ files from the 50 states of the United States (READ et al., 2017). The rapid growth of these portals is likely to be a major contribution to WQ models in the near future.

## 5 LIMITATIONS

Remote sensing offers a number of advantages to estimate WQ in lakes and reservoirs. The spatio-temporal coverage, the analysis of bodies of water inaccessible to man, the rapid data acquisition and the recovery of historical data through time series are some of these advantages (ANSPER; ALIKAS, 2019; ZHAO et al., 2020; TOPP et al., 2020). However, it is worthwhile mentioning the existence of restrictions that are inherent to its application. The dependence on good climatic conditions, as well as the spatial and temporal variation of air masses and solar illumination can be considered limiting factors (ANSPER; ALIKAS, 2019). The optical image products may present atmospheric interference capable of negatively affecting or even

preclude the results (VERONEZ et al., 2018).

The spatial resolution of images can also be a limiting factor for small lakes, ponds and small reservoirs. Images of low or moderate resolution like MODIS (250 – 1000 m), Sentinel-3/OLCI (300 m) or Proba-V (300 – 600 m) can have very limited application for water bodies smaller than 2500 km<sup>2</sup> due to the large number of pixels with a mixture of land and water (MERTES et al., 2004; CUI et al., 2013; VERONEZ et al., 2018). Likewise, sensors with low spectral resolution might not be appropriate for monitoring WQ parameters which can be related to very specific portions of the electromagnetic spectrum. It is the case of PC for example, which shows a narrow absorption peak around 620 nm (OGASHAWARA, 2019) or the chl-a which is better quantified with sensors having red-edge band ( $\approx$  690 – 740 nm). In addition, sensors of very high spatial resolution are mostly found in commercial satellites and can present a prohibitive cost for research in large lakes and reservoirs. The same applies to most hyperspectral sensors which are only available for aerial operations (with the possible exception of EO-1/Hyperion decommissioned March 2017).

The temporal resolution or revisit capacity is another factor that can prevent effective monitoring if the frequency desired is greater than the satellite revisit capacity or if the local atmospheric conditions do not allow clear sky often enough (VERONEZ et al., 2018). It might also be necessary to perform in situ measurement synchronised with the sensor overpass which can impose further restrictions (WILKIE et al., 2019).

Continental water bodies are often very complex and vary enormously from one region to the other. As such, it is generally inadvisable to compare concentrations measured through remote sensing from one water body to another since some algorithms demand to be calibrated locally and might not be replicable in other areas (ODERMATT et al., 2018) especially if these areas are distant and subjected to different environmental conditions. Concentrations of water constituents can be influenced by submersed vegetation or by other sources originating from the bottom and these can directly affect the radiance/reflectance at the surface and produce false estimates (CUI et al., 2013). Because remote sensing is limited to measurements in superficial waters, only three-dimensional models can help to explain the behaviour of these particles in suspension throughout the water column (MARKERT et al., 2018).

Some remote sensing results also strongly depend on local analysis. For example, it can be used to estimate the concentration and distribution of cyanobacteria but cannot identify their type or the number of different toxins they produce which is really what matters in terms of health hazard (VAN DER MERWE; PRICE, 2015). Similarly, if remote sensing can give good estimates of suspended solids, it does not directly inform about the transport dynamics (MARKERT et al., 2018).

At last, many important parameters cannot be measured directly simply because they do not affect the optical properties of water in the wavelengths (position and width) used by the available sensors. Although some success has been obtained in estimating these parameters because of their relationship with other OA parameters, these approaches are essentially empirical and a better understanding of these relations will require complex models involving many parameters, some of which might not be estimated through remote sensing.

## 6 CONCLUSIONS

Our review revealed that the past two decades have produced an exponentially growing mass of articles on the subject of remote sensing applied to the quantitative estimation of WQ parameters. A total of 127 articles were collected. We have concentrated our review on lentic environments (mostly lakes and reservoirs) for which there is a very wide range of platforms and sensors that covers from moderate spatial resolutions useful for large lakes and reservoirs to the very high- (< 1 m) and even ultra-high-resolutions (< 0.1 m) that can be achieved from commercial satellites.

Even though the empirical methods of correlation and regression still dominate broadly the range of approaches used, other more complex methods like neural network and deep learning are gaining terrain in terms of popularity. Analytical and semi-analytical approaches are also being used but in much lesser proportion. They are mainly applied to chl-a and Secchi disk depth and appear to achieve results comparable to empirical approaches. The important advantage of analytical approaches resides in their theoretical independence from in situ data once the model is calibrated and are more exportable to different environments, both timely and geographically. They do however, involve more control over the environmental variables



affecting the optical characteristics of water.

We also found that there is a general consensus in many articles in terms of the spectral bands used to model the parameters considered in this paper. In all cases wavelengths covered by the visible bands have a predominant role because of their ability to penetrate water and be sufficiently reflected or absorbed by exotic elements present within the first centimetres to few metres below the surface. The red band bears a significant importance, most notably for all optically active components (chl-a, SDD and turbidity). The blue band is more present for SDD and turbidity, but because the blue light is scattered about five times more than red (see Jensen (2005, p. 187)), atmospheric attenuation can be an issue with the blue band (TOMING et al., 2016). The near infrared is mostly used in chl-a models but usually in combination with one or more band in the visible spectrum.

One notable “newcomer” in the spectral band realm is the “red-edge” band ( $\approx 690 - 740$  nm) that first appeared in a civil satellite with the RapidEye constellation of five satellites (RapidEye Basic Product) launched in 2008. The red-edge band has proven to be good for chl-a but also for turbidity. Instruments on-board the Sentinel-2 and -3 satellites as well as some commercial VHR satellites (e.g., WorldView) all have one or more red-edge band. Another more subtle improvement that might have contributed in producing good results for many of the recent studies resides in the increase in spectral resolution of recent instruments on-board satellites. The Sentinel-2 (MSI instrument) and -3 (OLCI instrument) as well as Landsat-8 (OLI), RapidEye (REIS) and MODIS all have relatively narrower spectral bands than earlier satellite instruments. With the launch of many new satellites in the foreseeable future (Sentinel-2C/MSI, Sentinel-3C/OLCI, ResourceSat-3/ALISS III, Landsat-9/OLI-2, JPSS-2/VIIRS, HypSPIRI, EnMAP e PACE/OCI), these improvements are likely to continue.

Throughout this review, it stood out that the results can vary broadly in part because of the variety of instruments and approaches used. It also became clear through some articles that environmental factors such as season, atmospheric conditions, type and complexity of water can have an important effect on the quality of the results. It gives an indication on the kind of general results that can be expected. Chl-a for instance can yield results with much greater variation than SDD. It appears to be less reliable when the levels are very low. Our opinion after consulting over 180 articles, 143 of which we quoted, is that these environmental factors might be more determinant on the accuracy of the results than the actual approach used. The instruments used (satellite/sensor) is probably the next factor in importance with an emphasis on the wavelength and bandwidth of the spectral bands available. Conversely, because water is a poor reflector, the narrower the spectral band, the less energy is reflected back towards the sensor. This is a paradoxical limitation for which a solution strongly depends on technological advancements.

## **Acknowledgements**

This work was produced within the frame of a wider project entitled “Intelligent Water Quality Monitoring through the Development of Photo-optical Algorithm” and financed by the Companhia Energética de Minas Gerais (CEMIG, project GT-0607). The authors are most grateful to the GT-0607 Team who made this article possible.

## **Authors' Contribution**

The Fernanda Pizani (first author) was responsible for Conceptualization, Research and Methodology, Visualization and Writing – initial draft and editing. The Philippe Maillard (second author) was responsible for Conceptualization, Supervision and Writing – review and editing. The Camila Amorim (third author) was responsible for Conceptualization and Proofreading.

## **Conflict of interest**

The authors declared no potential conflicts of interest with respect to the research, authorship, and/or publication of this article.

## References

- ABDELMALIK, K. Role of statistical remote sensing for inland water quality parameters prediction. **The Egyptian Journal of Remote Sensing and Space Science**, v.21, n.2, p.193-200, September 2018, DOI. 10.1016/j.ejrs.2016.12.002.
- ALCÂNTARA, E.H.; STECH, J.L.; LORENZZETTI, J.A.; NOVO, E.M.L.M. Time series analysis of water surface temperature and heat flux components in the Itumbiara Reservoir (GO), Brazil. **Acta Limnologica Brasiliensia**, v.23, n.3, p.245-259, September 2011, DOI. 10.1590/S2179-975X2012005000002.
- ALPARSLAN, E.; COSKUN, H.G.; ALGANCI, U. Water quality determination of Küçükçekmece Lake, Turkey by using multispectral satellite data. **The Scientific World Journal**, v.9, p.1215-1229, November 2009, DOI. 10.1100/tsw.2009.135.
- ALPARSLAN, E.; COSKUN, H.G.; ALGANCI, U. An investigation on water quality of Darlik Dam drinking water using satellite images. **The Scientific World Journal**, v.10, 1293-1306, May 2010, DOI. 10.1100/tsw.2010.125.
- ALPAYDIN, E. **Introduction to machine learning**. 4ed. Cambridge, Massachusetts: The MIT Press, 2020.
- ANSPER, A.; ALIKAS, K. Retrieval of chlorophyll a from Sentinel-2 MSI data for the european union water framework directive reporting purposes. **Remote Sensing**, v.11, n.1, January 2019. DOI. 10.3390/rs11010064.
- AVDAN, Z.Y.; KAPLAN, G.; GONCU, S.; AVDAN, U. Monitoring the water quality of small water bodies using high-resolution remote sensing data. **ISPRS International Journal of Geo-Information**, v.8, n.12, December 2019. DOI. 10.3390/ijgi8120553.
- BARRETT, D.C.; FRAZIER, A.E. Automated method for monitoring water quality using Landsat imagery. **Water**, v.8, n.6, June 2016. DOI. 10.3390/w8060257.
- BINDING, C.; GREENBERG, T.; JEROME, J.; BUKATA, R.; LETOURNEAU, G. An assessment of MERIS algal products during an intense bloom in Lake of the Woods. **Journal of Plankton Research**, v.33, n.5, p.793-806, May 2011, DOI. 10.1093/plankt/fbq133.
- BINDING, C.; GREENBERG, T.; MCCULLOUGH, G.; WATSON, S.; PAGE, E. An analysis of satellite-derived chlorophyll and algal bloom indices on Lake Winnipeg. **Journal of Great Lakes Research**, v.44, n.3, p.436-446, June 2018. DOI. 10.1016/j.jglr.2018.04.001.
- BLIX, K.; PÁLFFY, K.; TÓTH, V.; ELTOFT, T. Remote sensing of water quality parameters over Lake Balaton by using Sentinel-3 OLCI. **Water**, v.10, n.10, October 2018, DOI. 10.3390/w10101428.
- BONANSEA, M.; BAZÁN, R.; LEDESMA, C.; RODRIGUEZ, C.; PINOTTI, L. Monitoring of regional lake water clarity using Landsat imagery. **Hydrology Research**, v.46, n.5, p.661-670, October 2015, DOI. 10.2166/nh.2014.211.
- BONANSEA, M.; RODRIGUEZ, C.; PINOTTI, L. Assessing the potential of integrating Landsat sensors for estimating chlorophyll-a concentration in a reservoir. **Hydrology Research**, v.49, n.5, p.1608-1617, October 2018. DOI. 10.2166/nh.2017.116.
- BRESCIANI, M.; CAZZANIGA, I.; AUSTONI, M.; SFORZI, T.; BUZZI, F.; MORABITO, G.; GIARDINO, C. Mapping phytoplankton blooms in deep subalpine lakes from Sentinel-2A and Landsat-8. **Hydrobiologia**, v.824, p.197-214, January 2018, DOI. 10.1007/s10750-017-3462-2.
- BRESCIANI, M.; PINARDI, M.; FREE, G.; LUCIANI, G.; GHEBREHIWOT, S.; LAANEN, M.; PETERS, S.; DELLA BELLA, V.; PADULA, R.; GIARDINO, C. The use of multisource optical sensors to study phytoplankton spatio-temporal variation in a shallow turbid lake. **Water**, v.12, n.1, January 2020. DOI. 10.3390/w12010284.
- CABALLERO, I.; NAVARRO, G. Monitoring cyanoHABs and water quality in Laguna Lake (Philippines) with Sentinel-2 satellites during the 2020 Pacific typhoon season. **Science of The Total Environment**, v.788, September 2021, DOI. 10.1016/j.scitotenv.2021.147700.

- CAO, Z.; MA, R.; DUAN, H.; XUE, K.; SHEN, M. Effect of satellite temporal resolution on long-term suspended particulate matter in inland lakes. **Remote Sensing**, v.11, n.23, November 2019. DOI. 10.3390/rs11232785.
- CGLS – Copernicus Global Land Service. **Lake Water Quality**. Available at: <<https://land.copernicus.eu/global/products/lwq>>. Accessed in: 20 Dec. 2021.
- CHEN, F.; WU, G.; WANG, J.; HE, J.; WANG, Y. A MODIS-based retrieval model of suspended particulate matter concentration for the two largest freshwater lakes in China. **Sustainability**, v.8, n.8, August 2016. DOI. 10.3390/su8080832.
- CHENG, C.; WEI, Y.; LV, G.; YUAN, Z. Remote estimation of chlorophyll- a concentration in turbid water using a spectral index: a case study in Taihu Lake, China. **Journal of Applied Remote Sensing**, v.7, n.1, December 2013. DOI. 10.1117/1.JRS.7.073465.
- COELHO, C.; HEIM, B.; FOERSTER, S.; BROSINSKY, A.; ARAÚJO, J.C. In situ and satellite observation of CDOM and chlorophyll-a dynamics in small water surface reservoirs in the Brazilian semiarid region. **Water**, v.9, n.12, December 2017. DOI. 10.3390/w9120913.
- COELHO, L.S.; ROCHE, K.F.; PARANHOS FILHO, A.C.; LEMOS, V.B. Uso do sensor CBERS/CCD na avaliação do estado trófico do Reservatório Lago do Amor (Campo Grande, MS). **Revista Brasileira de Cartografia**, v.63, n.2, p.221-232, 2011.
- CUI, L.; QIU, Y.; FEI, T.; LIU, Y.; WU, G. Using remotely sensed suspended sediment concentration variation to improve management of Poyang Lake, China. **Lake and Reservoir Management**, v.29, n.1, p.47-60, February 2013. DOI. 10.1080/10402381.2013.768733.
- CURTARELLI, M.; ALCÂNTARA, E.; RENNÓ, C.; STECH, J. Physical changes within a large tropical hydroelectric reservoir induced by wintertime cold front activity. **Hydrology and Earth System Sciences**, v.18, n.8, p.3079-3093, August 2014. DOI. 10.5194/hess-18-3079-2014.
- DOXANI, G.; VERMOTE, E.; ROGER, J.C.; GASCON, F.; ADRIAENSEN, S.; FRANTZ, D.; HAGOLLE, O.; HOLLSTEIN, A.; KIRCHES, G.; LI, F.; LOUIS, J.; MANGIN, A.; PAHLEVAN, N.; PFLUG, B.; VANHELLEMONT, Q. Atmospheric correction inter-comparison exercise. **Remote Sensing**, v.10, n.2, February 2018. DOI. 10.3390/rs10020352.
- ELHAG, M.; GITAS, I.; OTHMAN, A.; BAHRAWI, J.; GIKAS, P. Assessment of water quality parameters using temporal remote sensing spectral reflectance in arid environments, Saudi Arabia. **Water**, v.11, n.3, March 2019. DOI. 10.3390/w11030556.
- EUGENIO, F.; MARCELLO, J.; MARTÍN, J. Multiplatform earth observation systems for monitoring water quality in vulnerable inland ecosystems: Maspalomas Water Lagoon. **Remote Sensing**, v.12, n.2, January 2020. DOI. 10.3390/rs12020284.
- FACCO, D.S.; GUASSELLI, L.A.; RUIZ, L.F.C.; SIMIONI, J.P.D.; DICK, D.G. Spectral reflectance in the spatial-temporal dynamic of turbidity, Itaipu Reservoir, Brazil. **Anuário do Instituto de Geociências**, v.44, n.41228, 2021. DOI. 10.11137/1982-3908\_2021\_44\_41228.
- FERREIRA, M.S.; GALO, M.L.B. Chlorophyll a spatial inference using artificial neural network from multispectral images and in situ measurements. **Anais da Academia Brasileira de Ciências**, v.85, n.2, p.519-532, June 2013. DOI. 10.1590/S0001-37652013005000037.
- FLORES-ANDERSON, A.I.; GRIFFIN, R.; DIX, M.; ROMERO-OLIVA, C.S.; OCHAETA, G.; SKINNER-ALVARADO, J.; RAMIREZ MORAN, M.V.; HERNANDEZ, B.; CHERRINGTON, E.; PAGE, B.; BARRENO, F. Hyperspectral satellite remote sensing of water quality in Lake Atitlán, Guatemala. **Frontiers in Environmental Science**, v.8, February 2020. DOI. 10.3389/fenvs.2020.00007.
- GHOLIZADEH, M.H.; MELESSE, A.M.; REDDI, L. A comprehensive review on water quality parameters estimation using remote sensing techniques. **Sensors**, v.16, n.8, August 2016. DOI. 10.3390/s16081298.
- GIARDINO, C.; BRESCIANI, M.; CAZZANIGA, I.; SCHENK, K.; RIEGER, P.; BRAGA, F.; MATTA, E.; BRANDO, V.E. Evaluation of multi-resolution satellite sensors for assessing water quality and bottom depth of Lake Garda. **Sensors**, v.14, n.12, p.24116-24131, December 2014. DOI. 10.3390/s141224116.

- GORELICK, N.; HANCHER, M.; DIXON, M.; ILYUSHCHENKO, S.; THAU, D.; MOORE, R. Google Earth Engine: Planetary-scale geospatial analysis for everyone. **Remote sensing of Environment**, v.202, p.18-27, December 2017. DOI. 10.1016/j.rse.2017.06.031.
- HA, N.T.T.; THAO, N.T.P.; KOIKE, K.; NHUAN, M.T. Selecting the best band ratio to estimate chlorophyll-a concentration in a tropical freshwater lake using Sentinel 2A images from a case study of Lake Ba Be (Northern Vietnam). **ISPRS International Journal of Geo-Information**, v.6, n.9, September 2017. DOI. 10.3390/ijgi6090290.
- HAFEEZ, S.; WONG, M.S.; HO, H.C.; NAZEER, M.; NICHOL, J.; ABBAS, S.; TANG, D.; LEE, K.H.; PUN, L. Comparison of machine learning algorithms for retrieval of water quality indicators in case-II waters: a case study of Hong Kong. **Remote Sensing**, v.11, n.6, p.617, March 2019. DOI. 10.3390/rs11060617.
- HANSEN, C.H.; WILLIAMS, G.P. Evaluating remote sensing model specification methods for estimating water quality in optically diverse lakes throughout the growing season. **Hydrology**, v.5, n.4, November 2018, DOI. 10.3390/hydrology5040062.
- HEAL, K.V.; BARTOSOVA, A.; HIPSEY, M.R.; CHEN, X.; BUYTAERT, W.; LI, H.Y.; MCGRANE, S.J.; GUPTA, A.B.; CUDENNEC, C. Water quality: the missing dimension of water in the water-energy-food nexus. **Hydrological Sciences Journal**, v.66, n.5, p.745-758, March 2021. DOI. 10.1080/02626667.2020.1859114.
- HUO, A.; ZHANG, J.; QIAO, C.; LI, C.; XIE, J.; WANG, J.; ZHANG, X. Multispectral remote sensing inversion for city landscape water eutrophication based on genetic algorithm-support vector machine. **Water Quality Research Journal of Canada**, v.49, n.3, p.285-293, August 2014. DOI. 10.2166/wqrjc.2014.040.
- JENSEN, J.R. **Introductory digital image processing: a remote sensing perspective**. 3ed. Upper Saddle River: Prentice-Hall, 2005
- KIM, Y.H.; IM, J.; HA, H.K.; CHOI, J.K.; HA, S. Machine learning approaches to coastal water quality monitoring using GOCI satellite data. **GIScience & Remote Sensing**, v.51, n.2, p.158-174, April 2014. DOI. 10.1080/15481603.2014.900983.
- KNIGHT, J.F.; VOTH, M.L. Application of MODIS imagery for intra-annual water clarity assessment of Minnesota lakes. **Remote Sensing**, v.4, n.7. p.2181-2198, July 2012. DOI. 10.3390/rs4072181.
- KUMAR, L.; MUTANGA, O. Google Earth Engine applications since inception: usage, trends, and potential. **Remote Sensing**, v.10, n.10, September 2018. DOI. doi.org/10.3390/rs10101509.
- KUPSSINSKÜ, L.S.; GUIMARÃES, T.T.; SOUZA, E.M.; ZANOTTA, D.C.; VERONEZ, M.R.; GONZAGA, L.; MAUAD, F.F. A method for chlorophyll-a and suspended solids prediction through remote sensing and machine learning. **Sensors**, v.20, n.7, April 2020. DOI. 10.3390/s20072125.
- LARY, D.J.; ALAVI, A.H.; GANDOMI, A.H.; WALKER, A.L. Machine learning in geosciences and remote sensing. **Geoscience Frontiers**, v.7, n.1, p.3-10, January 2016. DOI. 10.1016/j.gsf.2015.07.003.
- LI, X.; HUANG, M.; WANG, R. Numerical simulation of Donghu Lake hydrodynamics and water quality based on remote sensing and MIKE 21. **ISPRS International Journal of Geo-Information**, v.9, n.2, February 2020. DOI. doi.org/10.3390/ijgi9020094.
- LI, Y.; TIAN, L.; LI, W.; LI, J.; WEI, A.; LI, S.; TONG, R. Design and experiments of a water color remote sensing-oriented unmanned surface vehicle. **Sensors**, v.20, n.8, April 2020. DOI. 10.3390/s20082183.
- LI, Y.; ZHANG, Q.; ZHANG, L.; TAN, Z.; YAO, J. Investigation of water temperature variations and sensitivities in a large floodplain lake system (Poyang Lake, China) using a hydrodynamic model. **Remote Sensing**, v.9, n.12, November 2017. DOI. 10.3390/rs9121231.
- LIN, S.; NOVITSKI, L.N.; QI, J.; STEVENSON, R.J. Landsat TM/ETM+ and machine-learning algorithms for limnological studies and algal bloom management of inland lakes. **Journal of Applied Remote Sensing**, v.12, n.2, April 2018. DOI. 10.1117/1.JRS.12.026003.
- LIU, D.; DUAN, H.; LOISELLE, S.; HU, C.; ZHANG, G.; LI, J.; YANG, H.; THOMPSON, J.R.; CAO, Z.; SHEN, M.; MA, R.; ZHANG, M.; HAN, W. Observations of water transparency in China's lakes from

- space. **International Journal of Applied Earth Observation and Geoinformation**, v.92, October 2020. DOI. 10.1016/j.jag.2020.102187.
- LIU, J.; ZHANG, Y.; YUAN, D.; SONG, X. Empirical estimation of total nitrogen and total phosphorus concentration of urban water bodies in China using high resolution IKONOS multispectral imagery. **Water**, v.7, n.11, p.6551-6573, November 2015. DOI. 10.3390/w7116551.
- LIU, X.; LEE, Z.; ZHANG, Y.; LIN, J.; SHI, K.; ZHOU, Y.; QIN, B.; SUN, Z. Remote sensing of Secchi depth in highly turbid lake waters and its application with MERIS data. **Remote Sensing**, v.11, n.19, September 2019. DOI. 10.3390/rs11192226.
- LIU, Y.; ISLAM, M.A.; GAO, J. Quantification of shallow water quality parameters by means of remote sensing. **Progress in Physical Geography**, v.27, n.1, p.24-43, March 2003. DOI. 10.1191/0309133303pp357ra.
- LOBO, F.L.; NAGEL, G.W.; MACIEL, D.A.; CARVALHO, L.A.S.; MARTINS, V.S.; BARBOSA, C.C.F.; NOVO, E.M.L.M. AlgaeMAP: Algae bloom monitoring application for inland waters in Latin America. **Remote Sensing**, v.13, n.15, July 2021. DOI. 10.3390/rs13152874.
- LUZ, G.A.; GUASSELLI, L.A.; ROCHA, D. Temperature surface of Guaíba Lake, RS, from time series of MODIS images. **Revista Brasileira de Recursos Hídricos**, v.22, n.17, November 2016. DOI. 10.1590/2318-0331.011716094.
- MACIEL, D.A.; BARBOSA, C.C.F.; NOVO, E.M.L.M.; FLORES-JÚNIOR, R.F.; BEGLIOMINI, F.N. Water clarity in Brazilian water assessed using Sentinel-2 and machine learning methods. **ISPRS Journal of Photogrammetry and Remote Sensing**, v.182, p.134-152, December 2021. DOI. 10.1016/j.isprsjprs.2021.10.009.
- MALAHLELA, O.E.; OLIPHANT, T.; TSOELENG, L.T.; MHANGARA, P. Mapping chlorophyll-a concentrations in a cyanobacteria- and algae-impacted Vaal Dam using Landsat 8 OLI data. **South African Journal of Science**, v.114, n.9/10, p.1-9, September/October 2018. DOI. 10.17159/sajs.2018/4841.
- MANCINO, G., NOLÈ, A., URBANO, V., AMATO, M., FERRARA, A., 2009. Assessing water quality by remote sensing in small lakes: the case study of Monticchio lakes in southern Italy. **iForest-Biogeosciences and Forestry**, v.2, n.1, p.154-161, July 2009. DOI. 10.3832/ifor0507-002.
- MARKELIN, L.; SIMIS, S.G.; HUNTER, P.D.; SPYRAKOS, E.; TYLER, A.N.; CLEWLEY, D.; GROOM, S. Atmospheric correction performance of hyperspectral airborne imagery over a small eutrophic lake under changing cloud cover. **Remote Sensing**, v.9, n.1, January 2017. DOI. 10.3390/rs9010002.
- MARKERT, K.N.; SCHMIDT, C.M.; GRIFFIN, R.E.; FLORES, A.I.; POORTINGA, A.; SAAH, D.S.; MUENCH, R.E.; CLINTON, N.E.; CHISHTIE, F.; KITYUTTACHAI, K. SOMETH, P.; ANDERSON, E.; AEKAKKARARUNGROJ, A.; GANZ, D. Historical and operational monitoring of surface sediments in the lower Mekong Basin using Landsat and Google Earth Engine cloud computing. **Remote Sensing**, v.10, n.6, June 2018. DOI. 10.3390/rs10060909.
- MARKOGIANNI, V.; KALIVAS, D.; PETROPOULOS, G.P.; DIMITRIOU, E. An appraisal of the potential of Landsat 8 in estimating chlorophyll-a, ammonium concentrations and other water quality indicators. **Remote Sensing**, v.10, n.7, June 2018. DOI. 10.3390/rs10071018.
- MENKEN, K.D.; BREZONIK, P.L.; BAUER, M.E. Influence of chlorophyll and colored dissolved organic matter (CDOM) on lake reflectance spectra: Implications for measuring lake properties by remote sensing. **Lake and Reservoir Management**, v.22, n.3, p.179-190, 2006. DOI. 10.1080/07438140609353895.
- MERTES, L.A.; DEKKER, A.; BRAKENRIDGE, G.; BIRKETT, C.; LETOURNOU, G. Rivers and lakes. In: USTIN, S.L. (Ed.). **Remote sensing for natural resource management and environmental monitoring**. 3ed. New York: John Wiley and Sons, 2004. p.345-400.
- MISHRA, M.K.; RATHORE, P.S.; MISRA, A.; KUMAR, R. Atmospheric correction of multi-spectral VNIR remote sensing data: Algorithm and inter-sensor comparison of aerosol and surface reflectance products. **Earth and Space Science**, v.7, n.9, April 2020. DOI. 10.1029/2019EA000710.
- MISHRA, S.; MISHRA, D. A novel remote sensing algorithm to quantify phycocyanin in cyanobacterial algal

- blooms. **Environmental Research Letters**, v.9, n.11, November 2014. DOI. 10.1088/1748-9326/9/11/114003.
- NEIL, C.; SPYRAKOS, E.; HUNTER, P.D.; TYLER, A.N. A global approach for chlorophyll-a retrieval across optically complex inland waters based on optical water types. **Remote Sensing of Environment**, v.229, p.159-178, August 2019. DOI. 10.1016/j.rse.2019.04.027.
- NOVO, E.M.L.M.; LONDE, L.R.; BARBOSA, C.; ARAUJO, C.A.; RENNÓ, C.D. Proposal for a remote sensing trophic state index based upon Thematic Mapper/Landsat images. **Revista Ambiente & Água**, v.8, n.3, p.65-82, December 2013. DOI. 10.4136/1980-993X.
- ODERMATT, D.; DANNE, O.; PHILIPSON, P.; BROCKMANN, C. Diversity II water quality parameters from ENVISAT (2002-2012): a new global information source for lakes. **Earth System Science Data**, v.10, n.3, August 2018. DOI. 10.5194/essd-10-1527-2018.
- ODERMATT, D.; HEEGE, T.; NIEKE, J.; KNEUBÜHLER, M.; ITTEN, K. Water quality monitoring for Lake Constance with a physically based algorithm for MERIS data. **Sensors**, v.8, n.8, p.4582-4599, August 2008. DOI. 10.3390/s8084582.
- OGASHAWARA, I. The use of Sentinel-3 imagery to monitor cyanobacterial blooms. **Environments**, v.6, n.6, June 2019. DOI. 10.3390/environments6060060.
- OGASHAWARA, I.; ALCÂNTARA, E.H.; CURTARELLI, M.P.; ADAMI, M.; NASCIMENTO, R.F.; SOUZA, A.F.; STECH, J.L.; KAMPEL, M. Performance analysis of MODIS 500-m spatial resolution products for estimating chlorophyll-a concentrations in oligo-to meso-trophic waters case study: Itumbiara Reservoir, Brazil. **Remote Sensing**, v.6, n.2, p.1634-1653, February 2014a, DOI. 10.3390/rs6021634.
- OGASHAWARA, I.; ALCÂNTARA, E.H.; STECH, J.L.; TUNDISI, J.G. Cyanobacteria detection in Guarapiranga Reservoir (São Paulo state, Brazil) using Landsat TM and ETM+ images. **Revista Ambiente & Água**, v.9, p.224-238, June 2014b. DOI. 10.4136/ambi-agua.1327.
- OGASHAWARA, I.; MORENO-MADRIÑÁN, M.J. Improving inland water quality monitoring through remote sensing techniques. **ISPRS International Journal of Geo-Information**, v.3, n.4, p.1234-1255, November 2014. DOI. 10.3390/ijgi3041234.
- PAGE, B.P.; OLMANSON, L.G.; MISHRA, D.R. A harmonized image processing workflow using Sentinel-2/MSI and Landsat-8/OLI for mapping water clarity in optically variable lake systems. **Remote Sensing of Environment**, v.231, September 2019. DOI. 10.1016/j.rse.2019.111284.
- PAHLEVAN, N.; SMITH, B.; SCHALLES, J.; BINDING, C.; CAO, Z.; MA, R.; ALIKAS, K.; KANGRO, K.; GURLIN, D.; HÀ, N.; MATSUSHITA, B.; MOSES, W.; GREB, S.; LEHMANN, K.; ONDRUSEK, M.; OPPELT, N.; STUMPF, R. Seamless retrievals of chlorophyll-a from Sentinel-2 (MSI) and Sentinel-3 (OLCI) in inland and coastal waters: A machine-learning approach. **Remote Sensing of Environment**, v.240, April 2020. DOI. 10.1016/j.rse.2019.111604.
- PALMER, S.C.; HUNTER, P.D.; LANKESTER, T.; HUBBARD, S.; SPYRAKOS, E.; TYLER, A.N.; PRESING, M.; HORVATH, H.; LAMB, A.; BALZTER, H.; TÓTH, V. Validation of Envisat MERIS algorithms for chlorophyll retrieval in a large, turbid and optically-complex shallow lake. **Remote Sensing of Environment**, v.157, p.158-169, February 2015a. DOI. 10.1016/j.rse.2014.07.024.
- PALMER, S.C.; ODERMATT, D.; HUNTER, P.; BROCKMANN, C.; PRESING, M.; BALZTER, H.; TÓTH, V. Satellite remote sensing of phytoplankton phenology in Lake Balaton using 10 years of MERIS observations. **Remote Sensing of Environment**, v.158, p.441-452, March 2015b. DOI. 10.1016/j.rse.2014.11.021.
- PEPPA, M.; VASILAKOS, C.; KAVROUDAKIS, D. Eutrophication monitoring for Lake Pamvotis, Greece, using Sentinel-2 data. **ISPRS International Journal of Geo-Information**, v.9, n.3, February 2020. DOI. 10.3390/ijgi9030143.
- PHILIPSON, P.; KRATZER, S.; BEN MUSTAPHA, S.; STRÖMBECK, N.; STELZER, K. Satellite-based water quality monitoring in Lake Vänern, Sweden. **International Journal of Remote Sensing**, v.37, n.16, p.3938-3960, July 2016. DOI. 10.1080/01431161.2016.1204480.

- PINARDI, M.; FENOCCHI, A.; GIARDINO, C.; SIBILLA, S.; BARTOLI, M.; BRESCIANI, M. Assessing potential algal blooms in a shallow fluvial lake by combining hydrodynamic modelling and remote-sensed images. *Water*, v.7, n.5, p.1921-1942, April 2015. DOI. 10.3390/w7051921.
- PIZANI, F.M.; MAILLARD, P.; FERREIRA, A.F.; AMORIM, C.C. Estimation of water quality in a reservoir from Sentinel-2 MSI and Landsat-8 OLI sensors. *ISPRS Annals of the Photogrammetry, Remote Sensing and Spatial Information Sciences*, v.3, p.401-408, August 2020. DOI. 10.5194/isprs-annals-V-3-2020-401-2020.
- POLITI, E.; CUTLER, M.E.; ROWAN, J.S. Evaluating the spatial transferability and temporal repeatability of remote-sensing-based lake water quality retrieval algorithms at the European scale: a meta-analysis approach. *International Journal of Remote Sensing*, v.36, n.11, p.2995-3023, June 2015. DOI. 10.1080/01431161.2015.1054962.
- POTES, M.; COSTA, M.J.; SALGADO, R. Satellite remote sensing of water turbidity in Alqueva Reservoir and implications on lake modelling. *Hydrology & Earth System Sciences*, v.16, n.6, p.1623-1633, June 2012. DOI. 10.5194/hess-16-1623-2012.
- PU, F.; DING, C.; CHAO, Z.; YU, Y.; XU, X. Water-quality classification of inland lakes using Landsat8 images by convolutional neural networks. *Remote Sensing*, v.11, n.14, p.1674, July 2019. DOI. 10.3390/rs11141674.
- PYO, J.C.; LIGARAY, M.; KWON, Y.S.; AHN, M.H.; KIM, K.; LEE, H.; KANG, T.; CHO, S.B.; PARK, Y.; CHO, K.H. High-spatial resolution monitoring of phycocyanin and chlorophyll-a using airborne hyperspectral imagery. *Remote Sensing*, v.10, n.8, p.1180, July 2018. DOI. 10.3390/rs10081180.
- QUANG, N.H.; SASAKI, J.; HIGA, H.; HUAN, N.H. Spatiotemporal variation of turbidity based on Landsat 8 OLI in Cam Ranh Bay and Thuy Trieu Lagoon, Vietnam. *Water*, v.9, n.8, p.570, August 2017. DOI. 10.3390/w9080570.
- READ, E.K.; CARR, L.; DE CICCO, L.; DUGAN, H.A.; HANSON, P.C.; HART, J.A.; KREFT, J.; READ, J.S.; WINSLOW, L.A. Water quality data for national- scale aquatic research: The Water Quality Portal. *Water Resources Research*, v.53, n.2, p.1735-1745, January 2017. DOI. 10.1002/2016WR019993.
- ROBERT, E.; KERGOAT, L.; SOUMAGUEL, N.; MERLET, S.; MARTINEZ, J.M.; DIAWARA, M.; GRIPPA, M. Analysis of suspended particulate matter and its drivers in Sahelian ponds and lakes by remote sensing (Landsat and MODIS): Gourma Region, Mali. *Remote Sensing*, v.9, n.12, p.1272, December 2017. DOI. 10.3390/rs9121272.
- RODRIGUES, T.; ALCÂNTARA, E.; WATANABE, F.; IMAI, N. Retrieval of Secchi disk depth from a reservoir using a semi-analytical scheme. *Remote Sensing of Environment*, v.198, p.213-228, September 2017. DOI. 10.1016/j.rse.2017.06.018.
- ROSMORDUC, V.; BENVENISTE, J.; BRONER, O.; DINARDO, S.; LAURET, O.; MILAGRO, M.; PICOT, N.; AMBROZIO, A.; ESCOLÀ, R.; GARCIA-MONDEJAR, A.; SCHRAMA, E.; RESTANO, M.; TERRA-HOMEM, M. **Radar Altimetry Tutorial**. October 2018. Available at: <http://www.altimetry.info>. Accessed in: 20 Dec. 2021.
- RUESCAS, A.B., HIERONYMI, M., MATEO-GARCIA, G., KOPONEN, S., KALLIO, K., CAMPS-VALLS, G. Machine learning regression approaches for colored dissolved organic matter (CDOM) retrieval with S2-MSI and S3-OLCI simulated data. *Remote Sensing*, v.10, n.5, p.786, May 2018. DOI. 10.3390/rs10050786.
- RUSSELL, S., NORVIG, P. Learning from observation. IN: Russell, S., Norvig, P. (Eds.). **Artificial intelligence: a modern approach**. New Jersey: Prentice Hall, 1995. p.525-562.
- SABAT-TOMALA, A.; JAROCINSKA, A.M.; ZAGAJEWSKI, B.; MAGNUSZEWSKI, A.S.; SLAWIK, L.M.; OCHTYRA, A.; RACZKO, E.; LECHNIO, J.R. Application of HySpex hyperspectral images for verification of a two-dimensional hydrodynamic model. *European Journal of Remote Sensing*, v.51, n.1, p.637-649, May 2018. DOI. 10.1080/22797254.2018.1470905.
- SAGAN, V.; PETERSON, K.T.; MAIMAITIJANG, M.; SIDIKE, P.; SLOAN, J.; GREELING, B.A.;

- MAALOUF, S.; ADAMS, C. Monitoring inland water quality using remote sensing: potential and limitations of spectral indices, bio-optical simulations, machine learning, and cloud computing. **Earth-Science Reviews**, v.205, p.103187, June 2020. DOI. 10.1016/j.earscirev.2020.103187.
- SILVA, H.A.N.; NARANJO, P.G.V.; RODRIGUES, L.P.S.; ARAÚJO, D.M.; PIRES, Y.P. Prediction of some physico-chemical parameters of water in Alton Reservoir, Suffolk, England. **WSEAS Transactions on Environment and Development**, v.16, p.119-131, 2020. DOI. 10.37394/232015.2020.16.12.
- SOLA, I.; GARCÍA-MARTÍN, A.; SANDONÍS-POZO, L.; ÁLVAREZ-MOZOS, J.; PÉREZ-CABELLO, F.; GONZÁLEZ-AUDÍCANA, M.; LLOVERÍA, R.M. Assessment of atmospheric correction methods for Sentinel-2 images in Mediterranean landscapes. **International Journal of Applied Earth Observation and Geoinformation**, v.73, p.63-76, December 2018. DOI. 10.1016/j.jag.2018.05.020.
- SON, S., WANG, M., 2019. VIIRS-Derived water turbidity in the Great Lakes. **Remote Sensing**, v.11, n.12, p.1448, June 2019. DOI. 10.3390/rs11121448.
- SOOMETTS, T.; UUDEBERG, K.; JAKOVELS, D.; BRAUNS, A.; ZAGARS, M.; KUTSER, T. Validation and comparison of water quality products in Baltic lakes using Sentinel-2 MSI and Sentinel-3 OLCI data. **Sensors**, v.20, n.3, p.742, January 2020. DOI. 10.3390/s20030742.
- SÒRIA-PERPINYÀ, X.; VICENTE, E.; URREGO, P.; PEREIRA-SANDOVAL, M.; RUÍZ-VERDÚ, A.; DELEGIDO, J.; SORIA, J.M.; MORENO, J. Remote sensing of cyanobacterial blooms in a hypertrophic lagoon (Albufera of València, Eastern Iberian Peninsula) using multitemporal Sentinel-2 images. **Science of The Total Environment**, v.698, p.134305, January 2020. DOI. 10.1016/j.scitotenv.2019.134305.
- STEFLOULI, M.; CHAROU, E. Monitoring of transnational lakes using geomatic techniques: a case study for Prespa lakes. **International Journal of Design & Nature and Ecodynamics**, v.7, n.2, p.199-209, 2012. DOI. 10.2495/DNE-V7-N2-199-209.
- TOMING, K.; KUTSER, T.; LAAS, A.; SEPP, M.; PAAVEL, B.; NÖGES, T. First experiences in mapping lake water quality parameters with Sentinel-2 MSI imagery. **Remote Sensing**, v.8, n.8, p.640, August 2016. DOI. 10.3390/rs8080640.
- TOPP, S.N.; PAVELSKY, T.M.; JENSEN, D.; SIMARD, M.; ROSS, M.R.V. Research trends in the use of remote sensing for inland water quality science: Moving towards multidisciplinary applications. **Water**, v.12, n.1, p.169, January 2020. DOI. 10.3390/w12010169.
- TORBICK, N., CORBIERE, M. A multiscale mapping assessment of Lake Champlain cyanobacterial harmful algal blooms. **International Journal of Environmental Research and Public Health**, v.12, n.9, p.11560-11578, September 2015. DOI. 10.3390/ijerph120911560.
- TORBICK, N.; HESSION, S.; STOMMEL, E.; CALLER, T. Mapping amyotrophic lateral sclerosis lake risk factors across northern New England. **International Journal of Health Geographics**, v.13, n.1, January 2014. DOI. 10.1186/1476-072X-13-1.
- TORBICK, N.; ZINITI, B.; STOMMEL, E.; LINDER, E.; ANDREW, A.; CALLER, T.; HANEY, J.; BRADLEY, W.; HENEGAN, P.L.; SHI, X. Assessing cyanobacterial harmful algal blooms as risk factors for amyotrophic lateral sclerosis. **Neurotoxicity Research**, v.33, p.199-212, January 2018. DOI. 10.1007/s12640-017-9740-y.
- UNEP – UNITED NATIONS ENVIRONMENT PROGRAMME. Global Freshwater Quality Database GEMStat. Available at <https://gemstat.org/>. Accessed in: 20 Dec. 2021.
- UUDEBERG, K.; AAVASTE, A.; KÖKS, K.; ANSPER, A.; UUSÕUE, M.; KANGRO, K.; ANSKO, I.; LIGI, M.; TOMING, K.; REINART, A. Optical water type guided approach to estimate optical water quality parameters. **Remote Sensing**, v.12, n.6, p.931, March 2020. DOI. 10.3390/rs12060931.
- VAN DER MERWE, D.; PRICE, K.P. Harmful algal bloom characterization at ultra-high spatial and temporal resolution using small unmanned aircraft systems. **Toxins**, v.7, n.4, p.1065-1078, March 2015. DOI. 10.3390/toxins7041065.
- VAN NGUYEN, M.; LIN, C.H.; CHU, H.J.; JAELANI, L.M.; SYARIZ, M.A. Spectral feature selection optimization for water quality estimation. **International Journal of Environmental Research and**



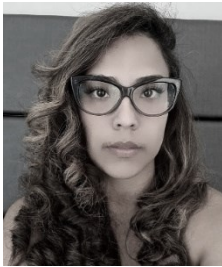
- Public Health**, v.17, n.1, p.272, January 2020. DOI. 10.3390/ijerph17010272.
- VERONEZ, M.R.; KUPSSINSKÛ, L.S.; GUIMARÃES, T.T.; KOSTE, E.C.; SILVA, J.M.; SOUZA, L.V.; OLIVERIO, W.F.; JARDIM, R.S.; KOCH, I.É.; SOUZA, J.G.; GONZAGA JUNIOR, L.; MAUAD, F.F.; INOCENCIO, L.C.; BORDIN, F. Proposal of a method to determine the correlation between total suspended solids and dissolved organic matter in water bodies from spectral imaging and artificial neural networks. **Sensors**, v.18, n.1, p.159, January 2018. DOI. 10.3390/s18010159.
- VERSCHUUR, G.L. Transparency measurements in Garner Lake, Tennessee: the relationship between Secchi depth and solar altitude and a suggestion for normalization of Secchi depth data. **Lake and Reservoir Management**, v.13, n.2, p.142-153, 1997. DOI. 10.1080/07438149709354305.
- VUNDO, A.; MATSUSHITA, B.; JIANG, D.; GONDWE, M.; HAMZAH, R.; SETIAWAN, F.; FUKUSHIMA, T. An overall evaluation of water transparency in Lake Malawi from MERIS data. **Remote Sensing**, v.11, n.3, p.279, January 2019. DOI. 10.3390/rs11030279.
- WANG, D.; KAGEYAMA, Y.; NISHIDA, M.; SHIRAI, H. Algorithm to analyze water quality conditions of Lake Hachiroko using textures of JERS-1 SAR data. **International Journal of the Society of Materials Engineering for Resources**, v.18, n.2, p.51-58, March 2012. DOI. 10.5188/ijmsmer.18.51.
- WANG, D.; KAGEYAMA, Y.; NISHIDA, M.; SHIRAI, H.; KASAI, C. Water quality analysis of Lake Hachiroko, Japan, using ALOS PALSAR data. **International Journal of the Society of Materials Engineering for Resources**, v.20, n.2, p.175-180, October 2014. DOI. 10.5188/ijmsmer.20.175.
- WANG, L.; XU, M.; LIU, Y.; LIU, H.; BECK, R.; REIF, M.; EMERY, E.; YOUNG, J.; WU, Q. Mapping freshwater chlorophyll-a concentrations at a regional scale integrating multi-sensor satellite observations with Google Earth Engine. **Remote Sensing**, v.12, n.20, p.3278, October 2020. DOI. 10.3390/rs12203278.
- WATANABE, F.; ALCANTARA, E.; RODRIGUES, T.; ROTTA, L.; BERNARDO, N.; IMAI, N. Remote sensing of the chlorophyll-a based on OLI/Landsat-8 and MSI/Sentinel-2A (Barra Bonita Reservoir, Brazil). **Anais da Academia Brasileira de Ciências**, v.90, p.1987-2000, August 2018. DOI. 10.1590/0001-3765201720170125.
- WATANABE, F.S.Y.; ALCÂNTARA, E.; RODRIGUES, T.W.P.; IMAI, N.N.; BARBOSA, C.C.F.; ROTTA, L.H.S. Estimation of chlorophyll-a concentration and the trophic state of the Barra Bonita Hydroelectric Reservoir using OLI/Landsat-8 images. **International Journal of Environmental Research and Public Health**, v.12, n.9, p.10391-10417, August 2015. DOI. 10.3390/ijerph120910391.
- WILKIE, C.J.; MILLER, C.A.; SCOTT, E.M.; O'DONNELL, R.A.; HUNTER, P.D.; SPYRAKOS, E.; TYLER, A.N. Nonparametric statistical downscaling for the fusion of data of different spatiotemporal support. **Environmetrics**, v.30, n.3, May 2019. DOI. 10.1002/env.2549.
- XIANG, B.; SONG, J.W.; WANG, X.Y.; ZHEN, J. Improving the accuracy of estimation of eutrophication state index using a remote sensing data-driven method: A case study of Chaohu Lake, China. **Water SA**, v.41, n.5, p.753-761, October 2015. DOI. 10.4314/WSA.V41I5.18.
- XIONG, J. ; LIN, C. ; MA, R. ; CAO, Z. Remote sensing estimation of lake total phosphorus concentration based on MODIS: A case study of Lake Hongze. **Remote Sensing**, v.11, n.17, p.2068, September 2019. DOI. 10.3390/rs11172068.
- XU, X.; HUANG, X.; ZHANG, Y.; YU, D. Long-term changes in water clarity in Lake Liangzi determined by remote sensing. **Remote Sensing**, v.10, n.9, p.1441, September 2018. DOI. 10.3390/rs10091441.
- ZENG, C.; BINDING, C. The effect of mineral sediments on satellite chlorophyll-a retrievals from line-height algorithms using red and near-infrared bands. **Remote Sensing**, v.11, n.19, p.2306, October 2019. DOI. 10.3390/rs11192306.
- ZHANG, M.; HU, C.; CANNIZZARO, J.; ENGLISH, D.; BARNES, B.B.; CARLSON, P.; YARBRO, L. Comparison of two atmospheric correction approaches applied to modis measurements over north american waters. **Remote Sensing of Environment**, v.216, p.442-455, October 2018. DOI. 10.1016/j.rse.2018.07.012.
- ZHANG, Y.; LIU, X.; QIN, B.; SHI, K.; DENG, J.; ZHOU, Y. Aquatic vegetation in response to increased

eutrophication and degraded light climate in Eastern Lake Taihu: Implications for lake ecological restoration. **Scientific Reports**, v.6, p.1-12, April 2016. DOI. 10.1038/srep23867.

ZHANG, Y.; WU, L.; REN, H.; DENG, L.; ZHANG, P. Retrieval of water quality parameters from hyperspectral images using Hybrid Bayesian Probabilistic Neural Network. **Remote Sensing**, v.12, n.10, p.1567, May 2020. DOI. 10.3390/rs12101567.

ZHAO, Y.; SHEN, Q.; WANG, Q.; YANG, F.; WANG, S.; LI, J.; ZHANG, F.; YAO, Y. Recognition of water colour anomaly by using hue angle and Sentinel 2 image. **Remote Sensing**, v.12, n.4, p.716, February 2020. DOI. 10.3390/rs12040716.

### First author biography



Fernanda Mara Coelho Pizani was born in Belo Horizonte-MG, Brazil, in 1986. She has a bachelor's degree in Geography from the Pontifical Catholic University of Minas Gerais (PUC-MG), and a master's degree in Analysis and Modeling of Environmental Systems from the Federal University of Minas Gerais (UFMG). She is currently a PhD candidate at the same institution and her research involves remote sensing applied to water quality.



Esta obra está licenciada com uma Licença [Creative Commons Atribuição 4.0 Internacional](https://creativecommons.org/licenses/by/4.0/) – CC BY. Esta licença permite que outros distribuam, remixem, adaptem e criem a partir do seu trabalho, mesmo para fins comerciais, desde que lhe atribuem o devido crédito pela criação original.